

Cadernos do LOGIS

Branch-and-cut-and-price for the robust
capacitated vehicle routing problem with
knapsack uncertainty

Artur Alves Pessoa, Michael Poss, Ruslan Sadykov, François
Vanderbeck

Volume 2018, Number 1

November, 2018



Branch-and-cut-and-price for the robust capacitated vehicle routing problem with knapsack uncertainty

Artur Alves Pessoa^a, Michael Poss^{b,*}, Ruslan Sadykov^c, François Vanderbeck^d

^a *Universidade Federal Fluminense, Rua Passo da Pátria, 156/309-D, Niterói – RJ, 24210-240, Brazil.*

^b *UMR CNRS 5506 LIRMM, Université de Montpellier, 161 rue Ada Montpellier, France.*

^c *INRIA Bordeaux - Sud-Ouest, 200 avenue de la Vieille Tour, 33405 Talence, France.*

^d *IMB, Université de Bordeaux, 351 cours de la Libération, 33405 Talence, France.*

Abstract

We examine the robust counterpart of the classical Capacitated Vehicle Routing Problem (CVRP). We consider two types of uncertainty sets for the customer demands: the classical budget polytope introduced by Bertsimas and Sim (2003), and a partitioned budget polytope proposed by Gounaris et al. (2013). We show that using the set-partitioning formulation it is possible to reformulate our problem as a deterministic heterogeneous vehicle routing problem. Thus, many state-of-the-art techniques for exactly solving deterministic VRPs can be applied for the robust counterpart, and a modern branch-and-cut-and-price algorithm can be adapted to our setting by keeping the number of pricing subproblems strictly polynomial. More importantly, we introduce new techniques to significantly improve the efficiency of the algorithm. We present analytical conditions under which a pricing subproblem is infeasible. This result is general and can be applied to other combinatorial optimization problems with knapsack uncertainty. We also introduce robust capacity cuts which are provably stronger than the ones known in the literature. Finally, a fast iterated local search algorithm is proposed to obtain heuristic solutions for the problem. Using our branch-and-cut-and-price algorithm incorporating existing and new techniques, we are able to solve to optimality all but one open instances from the literature.

Keywords: branch-and-cut-and-price, robust optimization, capacity inequalities, local search

1. Introduction

Vehicle routing problems (VRPs) form a highly studied class of combinatorial optimization problems with applications in a large number of fields, most often related to freight transportation and logistics. Vehicle routing concerns distribution of goods between depots and customers. Distribution is performed by vehicles which use a road network modeled as a graph. A solution of a VRP is a set of routes each performed by a vehicle starting and ending at its depot such

*Corresponding author

Email addresses: artur@producao.uff.br (Artur Alves Pessoa), michael.poss@lirmm.fr (Michael Poss), ruslan.sadykov@inria.fr (Ruslan Sadykov), francois.vanderbeck@math.u-bordeaux.fr (François Vanderbeck)

that operational constraints are satisfied, requirements of customers are fulfilled, and the transportation cost is minimized. A fundamental variant of VRP is the Capacitated Vehicle Routing Problem (CVRP), in which a unique product type is delivered from a single depot to customers using a fleet of identical vehicles. The only operational constraint here is that the total product demand of clients in a same route should not exceed the vehicle capacity.

The state-of-the-art approaches for exactly solving the CVRP and many other vehicle routing problems are based on branch-and-cut-and-price algorithms. These approaches formulate the problem using a set of binary variables, each of which is associated with the selection of a route that satisfies operational constraints. The number of such variables is usually exponential so that the linear relaxation of the formulation is solved by column generation. The pricing problem is a resource constrained elementary shortest path problem, typically solved by a labeling dynamic programming algorithm (Irnich and Desaulniers 2005). While already quite strong, the continuous relaxation of these formulations can be further reinforced using cutting planes (Fukasawa et al. 2006) and strong branching can be used to close the gap between the primal and dual bound if needed. Branch-and-cut-and-price algorithms have witnessed an important progress in the past 12 years: the bidirectional labeling algorithm was introduced by Righini and Salani (2006) to solve the pricing subproblem faster; an arc elimination by reduced costs (Irnich et al. 2010) was employed to reduce the size of the graph and to further speed up the labeling algorithm; *ng*-path relaxation (Baldacci et al. 2011) replaced the path elementarily requirement in pricing; route enumeration technique was suggested by Baldacci et al. (2008) in order to close the instance by a MIP solver when the primal-dual gap is sufficiently low; a limited memory technique for subset row cuts (Jepsen et al. 2008) and more generally for Chvatal-Gomory rank-1 cuts was proposed by Pecin et al. (2017b) for limiting the resulting solution time increase in the pricing subproblem.

The branch-and-cut-and-price algorithm of Pecin et al. (2017b), employing the aforementioned techniques, has proved that it was possible to solve exactly CVRPs much larger than ever before in reasonable amounts of time. Yet, it neglects to consider that the demands to be picked-up are rarely known with precision at the time the routes are planned. In the absence of a decision making tool modeling this uncertainty, decision makers are forced to largely overestimate the demands or to rely on expensive recourse actions to pick up the additional demands. Fortunately, different frameworks have arisen in the past decades to take such uncertainty into account when solving optimization problems, such as stochastic programming (Birge and Louveaux 2011), robust optimization (Ben-Tal et al. 2009, Ben-Tal and Nemirovski 1998, Kouvelis and Yu 2013), and more recently, distributionally robust optimization (Wiesemann et al. 2014). Stochastic variants of the CVRP have been extensively studied in the literature, see Gendreau et al. (1996) for an early survey and Dinh et al. (2018) for a more recent one and an advanced solution algorithm. Yet, these approaches result in optimization problems that tend to be significantly more complex than their deterministic counterparts, making them difficult to apply to large industrial applications. In addition, these techniques requires exact knowledge about the probability distributions of the

uncertain parameters, which can be hard to obtain in some applications.

Robust and distributionally robust counterparts of the CVRP avoid these two issues by describing the uncertain demands through either given uncertainty sets or probability distributions lying in given ambiguity sets. Hence, these approaches assume that only partial information about the distribution of the uncertain problem data is available. To our knowledge, the first study on the robust CVRP dates back to Sungur et al. (2008) who consider a variant of the robust CVRP where travel time is uncertain and the total travel time of each vehicle is bounded. They further study conditions under which all uncertain parameters reach simultaneously their extreme values, yielding a deterministic conservative reformulation. Their work was followed by the description of more general models in Ordóñez (2010). Later, Gounaris et al. (2013) study the robust CVRP and compare several compact mixed-integer formulations for the problems, including formulations involving recourse variables, modeled with the help of affine decision rules (Ben-Tal et al. 2004). Gounaris et al. (2013) also study the relationship between the robust CVRP and its chance-constrained distributionally robust counterpart. The latter problem is addressed more recently by Ghosal and Wiesemann (2018) where the authors characterize ambiguity sets that make the problem amenable to efficient numerical solutions. Heuristic algorithms have also been developed for the robust CVRP, among which Gounaris et al. (2016) who develop an adaptive memory programming framework for the problem.

This previous research studies have provided excellent exact or heuristic solutions to robust and distributionally robust CVRP, allowing one to solve larger instances than before. Yet, performance still stand significantly behind those offered by the recent algorithms for the deterministic CVRP (Pecin et al. 2017b). One theoretical reason explaining this difference lies in the complexity of robust optimization with arbitrary uncertainty sets. For instance, it is known that even optimizing a linear function over a robust knapsack constraint (an important substructure of the CVRP) is \mathcal{NP} -hard in the strong sense for arbitrary uncertainty sets (Talla Nobibon and Leus 2014), contrasting with the weak \mathcal{NP} -hardness of the deterministic case. In fact, it is well-known that arbitrary uncertainty sets make robust combinatorial optimization problems much harder than their deterministic counterparts, and most polynomially solvable problems become \mathcal{NP} -hard when considering robust variants with arbitrary uncertainty sets (Aissi et al. 2009).

This complexity gap has motivated the introduction of structured uncertainty sets that lead to robust counterparts almost as easy as the deterministic problems, namely, budgeted uncertainty sets (Bertsimas and Sim 2003). The latter models the uncertainty on demands through nominal values, deviations, and a budget of uncertainty. Then, any demand vector in the budgeted uncertainty polytope has a number of components that deviate from their mean that is controlled by the budget of uncertainty. Bertsimas and Sim (2003) prove that budgeted uncertainty leads to robust counterparts of min-max problem with cost uncertainty that are fundamentally as easy as the deterministic problems. Essentially, Bertsimas and Sim (2003) have shown that the optimal solution of a min-max combinatorial optimization problem with feasibility set $X \subseteq \{0, 1\}^n$ with

cost uncertainty can be obtained by solving n deterministic problems with perturbed cost vectors. Their results have been improved in subsequent works by Álvarez-Miranda et al. (2013), Lee and Kwon (2014), Lee et al. (2012) and extended to knapsack uncertainty sets by Poss (2018). While Bertsimas and Sim (2003) focused on cost uncertainty, Álvarez-Miranda et al. (2013) and Goetzmann et al. (2011) have independently shown how to extend these results to optimization problems with uncertain constraint parameters. In addition to its desirable computational properties, budgeted uncertainty sets also benefit from probabilistic guarantees, providing safe approximations to chance constraints (Bertsimas and Sim 2004, Poss 2013, 2014). Unfortunately, applying the above results to classical formulations of the CVRP with m vehicles would lead to solving $O(n^m)$ deterministic CVRP with perturbed data, explaining the current lack of interest in solving the robust CVRP with these techniques.

The main achievement of our present work is to bridge the gap between the advanced solution algorithms available for the deterministic CVRP and the iterative algorithms initiated by Bertsimas and Sim (2003). Specifically, we show that, by using the set-partitioning formulation, one can transpose all classical techniques of the CVRP to its robust counterpart. With that approach, we solve for the first time many instances proposed in the literature for the robust CVRP. In the process, we also introduce new techniques that apply to more general robust combinatorial optimization problems under knapsack uncertainty. We can summarize the contributions of our paper as follows.

1. We show how to reformulate the robust CVRP with knapsack uncertainty as a deterministic heterogeneous VRP that involves a polynomial number of pricing subproblems which are not harder than the pricing problem for the deterministic CVRP.
2. Using complementary slackness conditions, we can empirically verify that many pricing subproblems are infeasible, thus reducing their number. This technique can be applied to any robust combinatorial optimization problem with knapsack uncertainty.
3. We introduce new robust capacity inequalities and prove that they are stronger than those proposed by Gounaris et al. (2013).
4. We develop a fast iterated local search heuristic for the problem which uses four neighborhoods. We show how to check the feasibility of a neighbor either exactly or approximately in constant time. The heuristic is shown to empirically outperform the one by Gounaris et al. (2016).
5. Combining these new developments with a deterministic state-of-the-art branch-and-cut-and-price algorithm for the heterogeneous VRP, we are able to solve to proven optimality all but one instance for the partition uncertainty set considered previously by Gounaris et al. (2013).
6. We generate new robust CVRP instances for the classic cardinality constrained uncertainty set and show experimentally that they are more difficult than the ones proposed by Gounaris et al. (2013). The smallest open instance has only 50 customers.

The rest of the paper is structured as follows. Section 2 defines the uncertainty sets, states the extension of the the result from Bertsimas and Sim (2003) to knapsack uncertainty and provides extensions to reduce the number of problems solved. Section 3 describes the set-partitioning formulation that can be combined with the results from Section 2, and presents the key features of our branch-and-cut-and-price algorithm. Sections 4 and 5 detail our capacity inequalities and primal heuristics, respectively. The numerical experiments are presented in Section 6 and concluding remarks are provided in Section 7. Proofs, detailed numerical experiments, further examples and algorithmic specifications are deferred to the appendix. The latter also provides raw results to ease reproducibility of our experiments.

2. Robust model

Let $G = (V, A)$ be a complete digraph with nodes $V = \{0, 1, \dots, n\}$ and arcs $\{(i, j) \in V \times V : i \neq j\}$. Node $0 \in V$ represents the unique depot, and each node $i \in V^0 = V \setminus \{0\}$ corresponds to a customer with demand $d_i \in \mathbb{R}_+$. The depot hosts m homogeneous vehicles of capacity C . Each vehicle incurs a transportation cost $c_{ij} \in \mathbb{R}_+$ if it traverses the arc $(i, j) \in A$. The objective is to find a set of m routes starting and ending at the depot, each one serving a total demand of at most C , such that each customer is visited exactly once and the total transportation cost is minimized.

2.1. Uncertainty polytopes

The demand vector d can take any value in a given polytope \mathcal{D} that is included in the box $[\bar{d}, \bar{d} + \hat{d}]$ defined by the vectors $\bar{d}, \hat{d} \in \mathbb{R}_+^n$, where \bar{d} represent the nominal values and \hat{d} the deviations. Notice that it is irrelevant to consider downward deviations of d in our context because we focus on capacity constraints for which downward deviations of d will not lead to infeasibility of the constraints. We consider in this work two different polytopes. The first one is the budgeted polytope introduced in Bertsimas and Sim (2003, 2004), and widely used in the robust combinatorial optimization literature since then. Given $\Gamma \in \mathbb{R}_+$, the budgeted polytope is given by

$$\mathcal{D}^{card} = \left\{ d \in \mathbb{R}_+^n \mid d_i = \bar{d}_i + \eta_i \hat{d}_i, i \in V^0, \sum_{i \in V^0} \eta_i \leq \Gamma, 0 \leq \eta \leq 1 \right\}.$$

The second polytope we are interested in comes from Gounaris et al. (2013) where the authors consider a partition $V_C = \{V_1, \dots, V_s\}$ of V^0 and non-negative numbers $b_1, \dots, b_s \in \mathbb{R}_+$.

$$\mathcal{D}^{part} = \left\{ d \in \mathbb{R}_+^n \mid d_i = \bar{d}_i + \xi_i, i \in V^0, \sum_{i \in V_k} \xi_i \leq b_k, k = 1, \dots, s, 0 \leq \xi \leq \hat{d} \right\}.$$

To compare the two polytopes, one might use the relation $\xi_i = \hat{d}_i \eta_i$ which underlines the fact that \mathcal{D}^{card} constrains the number of elements of d that deviate simultaneously from their nominal values, while \mathcal{D}^{part} constrains the total amount of deviation for each partition of the uncertainty sources set. Restraining the total amount of deviation as in \mathcal{D}^{part} has been used in other contexts, such as robust scheduling in Tadayon and Smith (2015).

Let us consider a given combinatorial optimization problem \mathcal{P} . Further, let $Y \subseteq \{0, 1\}^n$ be a set of binary vectors such that the feasibility set of \mathcal{P} contains exactly the vectors in Y that also satisfies the following robust constraint

$$\sum_{i=1}^n (\bar{d}_i + \eta_i \hat{d}_i) y_i \leq C, \quad \forall \eta \in H, \quad (1)$$

where $H = \left\{ \eta \in [0, 1]^n \mid \sum_{i \in V_k} w_i \eta_i \leq b_k, k = 1, \dots, s \right\}$, where $w_i \geq 0$ for $i = 1, \dots, n$. In the context of the CVRP, \mathcal{P} decides which customers are visited by a given vehicle and each vector in Y represent a set of customers that could be visited by the vehicle.

Note that $\mathcal{D}^{knapp} = \{d \mid d_i = \bar{d}_i + \eta_i \hat{d}_i, \forall i \in \{1, \dots, n\}, \eta \in H\}$ generalizes both \mathcal{D}^{part} and \mathcal{D}^{card} . For the former, we set $w_i = \hat{d}_i$, and for the latter, $s = 1$, $b_1 = \Gamma$, and $w_1 = \dots = w_n = 1$. Note also that, assuming w.l.o.g. that $w_i > 0$ for $i = 1, \dots, n$, (1) is equivalent to

$$\bar{d}^\top y + \max_{\xi \in \Xi} \left\{ \sum_{i=1}^n \frac{\hat{d}_i}{w_i} \xi_i y_i \right\} \leq C, \quad (2)$$

where $\Xi = \left\{ \xi \in \mathbb{R}_+^n \mid \xi \leq w, \sum_{i \in V_k} \xi_i \leq b_k, k = 1, \dots, s \right\}$.

2.2. Reducing robust problems to deterministic ones

In the following, we give an alternative definition for (2) that helps to explore the ability to solve the deterministic counterpart of \mathcal{P} as a subproblem, and also allows us to reduce the solution space of the subproblems to be solved. For that, it is useful to rewrite (2) replacing the linear programming problem on its left-hand side by its dual:

$$\bar{d}^\top y + \min_{\theta, z \geq 0} \left\{ b^\top \theta + w^\top z \text{ s.t. } z_i + \theta_{k(i)} \geq \frac{\hat{d}_i}{w_i} y_i, \quad i = 1, \dots, n \right\} \leq C, \quad (3)$$

where $k(i)$ is the only value of k such that $i \in V_k$. By observing the one-to-one correspondence between the z variables and the constraints in (3), each z_i , for $i = 1, \dots, n$, can be replaced by $\max\{0, \frac{\hat{d}_i}{w_i} y_i - \theta_{k(i)}\}$. This leads to the equivalent constraint

$$\bar{d}^\top y + \min_{\theta \in \mathbb{R}_+^s} \left\{ b^\top \theta + \sum_{i=1}^n \max\{0, \hat{d}_i y_i - w_i \theta_{k(i)}\} \right\} = \bar{d}^\top y + \min_{\theta \in \mathbb{R}_+^s} \left\{ b^\top \theta + \sum_{i=1}^n \max\{0, \hat{d}_i - w_i \theta_{k(i)}\} y_i \right\}$$

$$= \min_{\theta \in \mathbb{R}_+^s} \left\{ b^\top \theta + \sum_{i=1}^n (\bar{d}_i + \max\{0, \hat{d}_i - w_i \theta_{k(i)}\}) y_i \right\} \leq C. \quad (4)$$

Now, let $d_i^\theta = \bar{d}_i + \max\{0, \hat{d}_i - w_i \theta_{k(i)}\}$, $Y^{knap} = \{y \in Y \mid d^\top y \leq C, \forall d \in \mathcal{D}^{knap}\}$, and $Y_\theta^{knap} = \{y \in Y \mid b^\top \theta + (d^\theta)^\top y \leq C\}$, for each $\theta \in \mathbb{R}_+^s$. Finally, let $\theta_k^0 = 0$ for $k = 1, \dots, s$, $\theta_{k(i)}^i = \hat{d}_i / w_i$ for $i = 1, \dots, n$, and

$$\Theta = (\{0\} \cup \{\theta_{k(i)}^i \mid i \in V_1\}) \times \dots \times (\{0\} \cup \{\theta_{k(i)}^i \mid i \in V_s\}). \quad (5)$$

The following theorem, the proof of which is deferred to Section Appendix A.1 of the appendix, requires that both \hat{d}_i and w_i are strictly greater than zero for $i = 1, \dots, n$. However, since they may be set as small as needed, this assumption is not restrictive from the practical point of view.

Theorem 1. $Y^{knap} = \bigcup_{\theta \in \Theta} Y_\theta^{knap}$

Theorem 1 shows that \mathcal{P} under the robust constraint (1) can be solved by taking the best solution among all instances of its deterministic counterpart generated using Y_θ^{knap} , for all $\theta \in \Theta$. The uncertainty sets covered by the theorem are more restricted than those studied in Theorem 3 from Poss (2018). This being said, the formula for Θ is simpler than the one from Poss (2018), which involves solving linear systems of equations. Notice also that the result has been known for a while in the case of \mathcal{D}^{card} (Álvarez-Miranda et al. 2013, Bertsimas and Sim 2003, Goetzmann et al. 2011, Lee and Kwon 2014), in which case $\Theta' = \{0, \hat{d}_1, \hat{d}_2, \dots, \hat{d}_n\}$. For the later set, Lee and Kwon (2014) further showed that only a subset of Θ' needs to be considered.

Theorem 2 (Lee and Kwon (2014)). *Consider \mathcal{D}^{card} and suppose w.l.o.g. that $\hat{d}_1 \geq \hat{d}_2 \geq \dots \geq \hat{d}_n \geq \hat{d}_{n+1} = 0$. Define $\Theta^{card} = \{\hat{d}_{\Gamma+1}, \hat{d}_{\Gamma+3}, \hat{d}_{\Gamma+5}, \dots, \hat{d}_{\Gamma+\gamma}, 0\}$ where γ is the largest odd integer such that $\Gamma + \gamma < n + 1$. It holds that for any $y \in \{0, 1\}^n$*

$$\operatorname{argmin}_{\theta \in \mathbb{R}_+^1} \left(\Gamma \theta + (\bar{d} + \max\{0, \hat{d} - \theta\})^\top y \right) \cap \Theta^{card} \neq \emptyset.$$

Defining $Y^{card} = \{y \in Y \mid d^\top y \leq C, \forall d \in \mathcal{D}^{card}\}$, and $Y_\theta^{card} = \{y \in Y \mid \Gamma \theta + (\bar{d} + \max\{0, \hat{d} - \theta\})^\top y \leq C\}$, for each $\theta \in \mathbb{R}_+^s$, Theorem 2 implies that the robust feasibility set Y^{card} can be reformulated as the union of the deterministic feasibility sets corresponding to the elements of $\Theta^{card} \subset \Theta$.

Corollary 1. $Y^{card} = \bigcup_{\theta \in \Theta^{card}} Y_\theta^{card}$

Let us turn to the implication of Theorem 1 to set \mathcal{D}^{part} . We see that applying formula (5) to \mathcal{D}^{part} leads to a set having a cardinality that no longer depends on n . Let $\Theta^{part} = \{0, 1\}^s$.

Lemma 1. *If $w_i = \hat{d}_i$ for each $i = 1, \dots, n$, then $\Theta = \Theta^{part}$.*

2.3. Reducing the cardinality of Θ

We explain next how to reduce even further the number of elements of Θ that need to be considered. Our approach works in two steps. First, we define

$$\tilde{Y}_\theta^{knap} = \left\{ y \in Y_\theta^{knap} \left| \begin{array}{l} \sum_{i \in V_k} w_i y_i \leq b_k, \forall k \in \{1, \dots, s\} \mid \theta_k = 0, \\ \sum_{\substack{i \in V_k \\ \hat{d}_i > w_i \theta_k}} w_i y_i \leq b_k \leq \sum_{\substack{i \in V_k \\ \hat{d}_i \geq w_i \theta_k}} w_i y_i, \forall k \in \{1, \dots, s\} \mid \theta_k > 0 \end{array} \right. \right\}.$$

We will show that one needs only to consider an element $\theta \in \Theta$ if \tilde{Y}_θ^{knap} is non-empty, by showing

$$\bigcup_{\theta \in \Theta} Y_\theta^{knap} = \bigcup_{\theta \in \Theta} \tilde{Y}_\theta^{knap}. \quad (6)$$

In fact, proving (6) would not be enough to cover Corollary 1 because the latter involves a proper subset $\Theta^{card} \subset \Theta$. Hence, the theorem below, the proof which is provided in Section Appendix A.2 of the appendix, generalizes slightly (6), by considering any set $\Theta^* \subseteq \Theta$ large enough to contain all minimizers of the left-hand side of (4).

Theorem 3. *Let $\Theta^* \subseteq \Theta$ be such that for each $y \in Y$*

$$\operatorname{argmin}_{\theta \in \mathbb{R}_+^s} \left(b^\top \theta + (d^\theta)^\top y \right) \cap \Theta^* \neq \emptyset. \quad (7)$$

Then, it holds that $\bigcup_{\theta \in \Theta^} Y_\theta^{knap} = \bigcup_{\theta \in \Theta^*} \tilde{Y}_\theta^{knap}$*

The constraints that are added in \tilde{Y}_θ^{knap} may destroy the structure of the original deterministic problem, making the corresponding optimization problem harder to solve. Here comes the second step of our approach: we use these constraints only to find out whether a given set \tilde{Y}_θ^{knap} is empty, in which case the corresponding θ can be removed from Θ^* . This is formalized in the next result.

Corollary 2. *Let $\Theta^* \subseteq \Theta$ that satisfies (7) and consider a set $\tilde{\Theta}$ such that $\{\theta \in \Theta^* \mid \tilde{Y}_\theta^{knap} \neq \emptyset\} \subseteq \tilde{\Theta}$. It holds that $Y^{knap} = \bigcup_{\theta \in \tilde{\Theta}} Y_\theta^{knap}$.*

For an arbitrary set Y , testing the emptiness of \tilde{Y}_θ^{knap} can be \mathcal{NP} -hard in the strong sense, so that we test instead the feasibility of a larger and simpler set. The later is defined by relaxing the combinatorial structure Y to $\{0, 1\}^n$ and removing the first two groups of constraints of \tilde{Y}_θ^{knap} .

Formally, we define $K(\theta) = \{k \in \{1, \dots, s\} \mid \theta_k > 0\}$, $\tilde{V}_k = \{i \in V_k \mid \hat{d}_i \geq w_i \theta_k\}$, and

$$\tilde{\mathbb{B}}_\theta^{knap} = \left\{ y \in \{0, 1\}^n \mid b^\top \theta + (d^\theta)^\top y \leq C, \sum_{i \in \tilde{V}_k} w_i y_i \geq b_k, \forall k \in K(\theta) \right\}.$$

Clearly, $\tilde{Y}_\theta^{knap} \subseteq \tilde{\mathbb{B}}_\theta^{knap}$. What is more, testing the emptiness of $\tilde{\mathbb{B}}_\theta^{knap}$ can be done by solving

$$\begin{aligned} z^* &= \min_{y \in \{0, 1\}^n} \left\{ (d^\theta)^\top y \mid \sum_{i \in \tilde{V}_k} w_i y_i \geq b_k, \forall k \in K(\theta) \right\} = \sum_{k \in K(\theta)} \min_{y \in \{0, 1\}^{|\tilde{V}_k|}} \left\{ \sum_{i \in \tilde{V}_k} d_i^\theta y_i \mid \sum_{i \in \tilde{V}_k} w_i y_i \geq b_k \right\} \\ &= \sum_{k \in K(\theta)} \min_{y \in \{0, 1\}^{|\tilde{V}_k|}} \left\{ \sum_{i \in \tilde{V}_k} d_i^\theta y_i \mid \sum_{i \in \tilde{V}_k} w_i y_i \geq b_k \right\}. \end{aligned}$$

Hence, z^* can be computed in pseudo-polynomial time by solving a knapsack problem for each $k \in K(\theta)$. If one of these knapsack problem is infeasible, then we set $z_k^* = \infty$. Then, having $z^* > C - b^\top \theta$ implies that $\tilde{\mathbb{B}}_\theta^{knap}$ is empty. For the special cases of \mathcal{D}^{card} and \mathcal{D}^{part} this computation is much simpler and can be done in a polynomial time as we show next.

Clearly, Θ^{card} satisfies (7) whenever $s = 1$, $b_1 = \Gamma$, and $w_1 = \dots = w_n = 1$, so that the Corollary 2 can be applied to reduce even further the number of elements considered both in Corollary 1 and Lemma 1. In this case, one can conclude that $\tilde{\mathbb{B}}_\theta^{knap}$ is empty (for $\theta > 0$) whenever

$$\min_{y \in \{0, 1\}^n} \left\{ \sum_{i \in \{1, \dots, n\} \mid \hat{d}_i \geq \theta} d_i^\theta y_i \mid \sum_{i \in \{1, \dots, n\} \mid \hat{d}_i \geq \theta} y_i = \Gamma \right\} > C - \Gamma \theta.$$

Note that the minimum is attained at the left-hand side of the previous inequality when $y_i = 1$ for the indices i that correspond to the Γ smallest values of \hat{d}_i that are not smaller than θ .

In the case of \mathcal{D}^{part} , we see that $\theta_{k(i)}^i = 1$, so that $\tilde{V}_k = V_k$ and $d_i^\theta = \bar{d}_i$. Now, we further assume that $\hat{d} = \kappa \bar{d}$ for some scalar $\kappa > 0$ (which is true for all current literature instances), and consider the linear relaxation of the counterpart of $\tilde{\mathbb{B}}_\theta^{knap}$ for \mathcal{D}^{part}

$$\tilde{\mathbb{I}}_\theta^{part} = \left\{ y \in [0, 1]^n \mid b^\top \theta + \bar{d}^\top y \leq C, \sum_{i \in V_k} \kappa \bar{d}_i y_i \geq b_k, \forall k \in K(\theta) \right\}.$$

Clearly, $\tilde{Y}_\theta^{part} \subseteq \tilde{\mathbb{I}}_\theta^{part}$. Further, $\min_{y \in [0, 1]^{|\tilde{V}_k|}} \left\{ \sum_{i \in \tilde{V}_k} \bar{d}_i y_i \mid \sum_{i \in \tilde{V}_k} \kappa \bar{d}_i y_i \geq b_k \right\} = b_k / \kappa$ for each $k \in K(\theta)$, so that the counterpart of z^* for \mathcal{D}^{part} is $(b^\top \theta) / \kappa$. Hence, $\tilde{\mathbb{I}}_\theta^{part}$ is necessarily empty when $(b^\top \theta) / \kappa > C - b^\top \theta$.

For both \mathcal{D}^{card} and \mathcal{D}^{part} , the set $\tilde{\Theta}$ can be computed in a pre-processing phase.

3. Set partitioning formulation and the solution algorithm

3.1. Deterministic problem

We describe in this section the set partitioning formulation used in our branch-and-cut-and-price algorithm. Let us start with the deterministic version of the problem and define R_0 as the set of all unconstrained elementary routes in G starting and ending at the depot. For each $r \in R_0$, we denote the cost of the route by c_r , and indicate whether node i (resp. arc (i, j)) pertains to the route by the binary number a_i^r (resp. δ_{ij}^r). Then, we describe the set of feasible routes for the CVRP with demand vector $\bar{d} \in \mathbb{R}_+^n$ as

$$R = \left\{ r \in R_0 \mid \sum_{i \in V_0} a_i^r \bar{d}_i \leq C \right\}.$$

The classical path formulation for the CVRP relies on a set of binary variables, denoted by λ , where λ_r is equal to 1 iff route r is part of the optimal solution. We obtain the following integer linear programming formulation

$$\min \sum_{r \in R} c_r \lambda_r, \quad (8)$$

$$\text{s.t.} \quad \sum_{r \in R} a_i^r \lambda_r = 1, \quad i \in V_0, \quad (9)$$

$$\sum_{r \in R} \lambda_r = m, \quad (10)$$

$$\lambda_r \in \mathbb{Z}, \quad r \in R, \quad (11)$$

In the above formulation, constraints (9) ensure that each customer is covered by exactly one vehicle, while constraint (10) sets the number of used vehicles to m .

The above integer program typically contains too many variables, so when solving this program by branch-and-bound, one generally solve the linear programming relaxation using a column generation procedure, i.e., generating the routes dynamically. Let $\tilde{R} \subseteq R$ be the set of routes generated so far, the restricted master linear program is obtained from (8)–(11) by replacing R with \tilde{R} . Given an optimal dual solution (π^*, σ^*) to the linear programming relaxation of (8)–(11) with \tilde{R} , where $\pi^* \in \mathbb{R}^n$ and $\sigma^* \in \mathbb{R}$, we generate new routes by solving the pricing problem

$$\min_{r \in R} c_r^*, \quad (12)$$

where $c_r^* = c_r - \sum_{i \in V_0} a_i^r \pi_i^* - m \sigma^*$.

3.2. Robust counterpart

When the demand of the clients can take any value in \mathcal{D}^{knap} , the set of feasible routes is reformulated as

$$R^{knap} = \left\{ r \in R_0 \left| \sum_{i \in V_0} a_i^r d_i \leq C, \quad \forall d \in \mathcal{D}^{knap} \right. \right\}.$$

Applying Corollary 2 to R^{knap} , we obtain

$$R^{knap} = \bigcup_{\theta \in \tilde{\Theta}} R^\theta, \quad (13)$$

where

$$R^\theta = \left\{ r \in R_0 \left| \sum_{i \in V_0} a_i^r d_i^\theta \leq C - b^\top \theta \right. \right\}.$$

Equation (13) underlines that the set of routes that are feasible for the robust capacity constraint is nothing else than the union of sets of routes feasible for different deterministic capacity constraints. Replacing R by R^{knap} in (8)–(11), and using (13), we obtain the path formulation for the robust CVRP

$$\min \sum_{\theta \in \tilde{\Theta}} \sum_{r \in R^\theta} c_r \lambda_r, \quad (14)$$

$$\text{s.t.} \quad \sum_{\theta \in \tilde{\Theta}} \sum_{r \in R^\theta} a_i^r \lambda_r = 1, \quad i \in V_0, \quad (15)$$

$$\sum_{\theta \in \tilde{\Theta}} \sum_{r \in R^\theta} \lambda_r = m, \quad (16)$$

$$\lambda_r \in \mathbb{Z}, \quad \theta \in \tilde{\Theta}, r \in R^\theta. \quad (17)$$

Similarly, the robust counterpart of the pricing problem (12) is

$$\min_{r \in R^{knap}} c_r^* = \min_{r \in \bigcup_{\theta \in \tilde{\Theta}} R^\theta} c_r^* = \min_{\theta \in \tilde{\Theta}} \min_{r \in R^\theta} c_r^*,$$

which can be decomposed into subproblems, one for each $\theta \in \tilde{\Theta}$.

3.3. branch-and-cut-and-price algorithm

To solve formulation (14)–(17), we adopt the branch-and-cut-and-price method by Sadykov et al. (2017) which is the state-of-the-art algorithm for the (heterogeneous) vehicle routing problem with time windows. The extension to our problem is the following: set of vehicle types here corresponds to set $\tilde{\Theta}$; vehicle type $\theta \in \tilde{\Theta}$ is characterized by specific vector d^θ of customer demands and vehicle capacity $C - b^\top \theta$; the limit m on the number of vehicles is global over all vehicle types; and there are no time windows. In the reminder of this subsection, we briefly

mention the techniques used in the algorithm. The reader is invited to read the original paper to obtain the detailed description.

In the algorithm, the linear relaxation of the formulation (14)–(17) is solved by column generation, stabilized using the automatic dual price smoothing technique by Pessoa et al. (2018). Each pricing subproblem $\theta \in \tilde{\Theta}$ is solved over the *ng*-path relaxation (Baldacci et al. 2011) of R^θ by the bi-directional bucket graph based labelling algorithm proposed by Sadykov et al. (2017). The main advantage of this labelling algorithm over another recent one by Pecin et al. (2017b) in our setting is that the former can take into account real-valued customer demands without negative impact on its performance. The *ng*-path relaxation is dynamically adjusted using the approach of Bulhoes et al. (2018). The bucket arcs in the bucket graphs are fixed using reduced cost arguments to simplify the pricing subproblems, as shown in Sadykov et al. (2017). We separate capacity cuts which are specific for the robust CVRP and which are presented below in Section 4. We also separate generic rank-1 Chvatal-Gomory cuts for up to 5 rows (Pecin et al. 2017a). Limited memory technique by Pecin et al. (2017b) is used to decrease the negative impact of rank-1 cuts on the difficulty of the pricing subproblems. Strong branching on edge variables is performed as in Pecin et al. (2017b). Elementary route enumeration procedure proposed by Baldacci et al. (2008) is employed to enumerate routes with reduced costs smaller than the current primal-dual gap. If the number of enumerated routes is small enough, the current branch-and-bound node is solved by the Cplex MIP solver. The initial feasible solution is obtained by the specific iterated local search heuristic which we describe in Section 5.

4. Capacity inequalities

Let x_{ij} be a binary variable equal to 1 iff there is a vehicle going through arc (i, j) . Then, for any subset of customers $S \subseteq V$, the rounded capacity inequalities, introduced by Laporte and Nobert (1983), state that the number of vehicles entering S must not be smaller than the total demand of the customers in S divided by the vehicle capacity. Stated formally for the robust problem, we obtain

$$\sum_{i \in V \setminus S} \sum_{j \in S} x_{ij} \geq \left\lceil \frac{1}{C} \max_{d \in \mathcal{D}} \sum_{i \in S} d_i \right\rceil, \quad S \subseteq V^0, \quad (18)$$

which has already been used by Gounaris et al. (2013) for the robust CVRP in the two-index vehicle flow formulation, here referred to as RVRP-2IF. The maximization over \mathcal{D} can be computed in polynomial time for both uncertainty polytopes considered. For \mathcal{D}^{card} , one must rely on a sorting algorithm that ranks the elements of $S \cap V_k$ according to the non-decreasing values of \hat{d}_i . For \mathcal{D}^{part} , the maximum can be directly computed as

$$\max_{d \in \mathcal{D}^{part}} \sum_{i \in S} d_i = \sum_{i \in S} \bar{d}_i + \sum_{k=1}^s \min \left\{ b_k, \sum_{i \in S \cap V_k} \hat{d}_i \right\}.$$

Notice finally that (18) can be written in terms of variables λ using the relation $x_{ij} = \sum_{\theta \in \tilde{\Theta}} \sum_{r \in R^\theta} \delta_{ij}^r \lambda_r$. We present next a reinforcement of the capacity inequalities.

Let $\tilde{r}(S)$ denote the right-hand side of (18), which is a lower bound on the number of vehicles required to serve all demand of vertices in S . We remark that the lower bound can be weak if many routes are used. To understand why, consider the following partition $S = S_1 \cup \dots \cup S_t$ and suppose that each route serves the nodes from one set of the partition. It holds that

$$\sum_{\ell=1}^t \max_{d \in \mathcal{D}} \sum_{i \in S_\ell} d_i \geq \max_{d \in \mathcal{D}} \sum_{i \in S} d_i,$$

and the inequality is likely to hold strictly. What is more, the difference between the two sides of the inequality tends to increase with the number of elements in the partition, therefore reducing the quality of the bound $\tilde{r}(S)$ when the number of routes used is large.

In order to strengthen (18), we define next a new lower bound $\dot{r}(S)$ on the number of routes required to visit S , which tends to be larger than $\tilde{r}(S)$ when t is large. Let us formulate the number of vehicles required to cover the customers of S as an integer program based on the reformulation (14)–(17). Specifically, we introduce the integer variable w_θ which represents how many vehicles of type θ are used, each of which having a capacity $C - b^\top \theta$, and the binary variable $v_{i\theta}$ which is equal to 1 iff customer i is affected to a vehicle of type θ (variables v can be related to variables λ used in (14)–(17) through $v_{i\theta} = \sum_{r \in R^\theta} a_i^r \lambda_r$). We obtain

$$\min \sum_{\theta \in \tilde{\Theta}} w_\theta, \tag{19}$$

$$\text{s.t. } \sum_{\theta \in \tilde{\Theta}} v_{i\theta} \geq 1, \quad i \in S, \tag{\mu_i} \tag{20}$$

$$\sum_{i \in S} d_i^\theta v_{i\theta} \leq (C - b^\top \theta) w_\theta, \quad \theta \in \tilde{\Theta}, \tag{\nu_\theta} \tag{21}$$

$$w_\theta \in \mathbb{Z}, \theta \in \tilde{\Theta}, v_{i\theta} \in \mathbb{Z}, i \in V, \theta \in \tilde{\Theta}. \tag{22}$$

where the corresponding dual variables of the continuous relaxation are denoted between parenthesis. In this formulation, (19) represents the minimum number of routes required to serve S , (20) ensures that every customer in S is served, and (21) avoids using more than the available capacity for each $\theta \in \tilde{\Theta}$. Solving (19)–(22) for each set S would provide the tightest value for the right-hand-side of (18). Solving all these integer programs is impractical so that we consider instead the values of the their continuous relaxation, which we denote $\dot{r}(S)$. Taking the dual of the continuous relaxation of (19)–(22), we obtain

$$\begin{aligned} \dot{r}(S) = \max \quad & \sum_{i \in S} \mu_i, \\ \text{s.t.} \quad & \mu_i \leq d_i^\theta \nu_\theta, \quad i \in S, \theta \in \tilde{\Theta}, \end{aligned}$$

$$(C - b^\top \theta) \nu_\theta \leq 1, \quad \theta \in \tilde{\Theta},$$

$$\mu, \nu \geq 0.$$

As a result, we have that

$$\hat{r}(S) = \sum_{i \in S} \min_{\theta \in \tilde{\Theta}} \frac{d_i^\theta}{C - b^\top \theta}. \quad (23)$$

We give in Section Appendix B of the appendix three examples that show that (24) improves upon (18) but there are cases where $\lceil \hat{r}(S) \rceil$ is smaller than $\tilde{r}(S)$. These examples show that the strongest capacity inequalities are given by

$$\sum_{i \in V \setminus S} \sum_{j \in S} x_{ij} \geq \max\{\lceil \hat{r}(S) \rceil, \tilde{r}(S)\} \quad S \subseteq V^0. \quad (24)$$

This being said, the advantage of using $\lceil \hat{r}(S) \rceil$ instead of the right-hand side of (24) is that the former allows to use the separation procedures proposed in Lysgaard et al. (2004), with modified demands. For that, each demand d_i is replaced by $\min_{\theta \in \tilde{\Theta}} \{d_i^\theta / (C - b^\top \theta)\}$, and the vehicle capacity is set to 1. Since the available implementation of this separation procedure requires that all demands and the vehicle capacity are integer, we multiply them by a large scale factor and round them properly to ensure the validity of the cuts. In practice, we have both types of separation procedures: one specialized in the separation of (24), and another one that uses the procedure of Lysgaard et al. (2004) and replaces the violated cuts by the equivalent ones of (24).

We conclude the section by showing how to further strengthen the proposed robust capacity cuts for the specific case of \mathcal{D}^{part} , with the additional assumption that the demand deviations are proportional to their nominal values. Namely, we assume that $\hat{d}_i = \kappa \bar{d}_i$ for all $i \in V^0$ for some $\kappa > 0$. The following theorem presents an even stronger version of the capacity inequalities; its proof and the proof of the subsequent proposition are provided in Sections Appendix A.3 and Appendix A.4 of the appendix.

Theorem 4. *The inequality $\sum_{i \in V \setminus S} \sum_{j \in S} x_{ij} \geq \hat{r}(S)$ is valid for the robust CVRP with \mathcal{D}^{part} , where*

$$\hat{r}(S) = \sum_{k=1}^s \left\lfloor \frac{q_k(S)}{\gamma_k} \right\rfloor + \left\lceil \sum_{k=1}^s \frac{\hat{q}_k(S) + \min\{b_k, \kappa \hat{q}_k(S)\}}{C} \right\rceil, \quad \gamma_k = \max\left\{\frac{C}{1+\kappa}, C - b_k\right\}, \quad q_k(S) = \sum_{i \in S \cap V_k} \bar{d}_i \text{ and}$$

$$\hat{q}_k(S) = q_k(S) - \gamma_k \left\lfloor \frac{q_k(S)}{\gamma_k} \right\rfloor \text{ for } k = 1, \dots, s.$$

Proposition 1. *$\hat{r}(S) \geq \max\{\lceil \hat{r}(S) \rceil, \tilde{r}(S)\}$ always holds and can be strict in some cases.*

We separate the robust capacity inequalities at each node of the branch-and-bound tree using a straightforward extension of the separation heuristic used in Uchoa et al. (2008). For completeness, its description in is provided Section Appendix C.1 of the appendix.

5. Heuristics

Efficient primal heuristics are usually required to provide good quality upper bounds on the optimal cost before running exact algorithms. For \mathcal{D}^{part} , Gounaris et al. (2016) proposed the AMP heuristic and showed that it helps the previously proposed branch-and-cut (BC) algorithm (Gounaris et al. 2013) to solve additional instances. Here, we develop an iterated local search (ILS) heuristic with variable neighborhood search (VNS) in the same spirit as Penna et al. (2013), which handles both \mathcal{D}^{part} and \mathcal{D}^{card} . This heuristic procedure is improved by a data structure specially designed to allow a faster evaluation of neighborhood solutions. In the next subsection, we show some properties of robust solutions explored by this data structure. Then, we give the full algorithm description in the subsection that follows.

5.1. Vehicle routing neighborhoods

A large number of neighborhoods known for vehicle routing problems (Vidal et al. 2013) can be extended to the robust CVRP. In this paper, we consider four neighborhoods: two intra-route and two inter-route. The intra-route neighborhoods are subpath inversions (2-OPT) and single customer moves between positions of the same route (reinsertion), and the inter-route ones are single-point crossovers of two routes (2-OPT*) and single customer moves from one route to another (insert). For all these neighborhoods, the cost of a neighbor solution can be evaluated in $O(1)$ time by updating the cost of the original solution considering only the costs of edges that change. For the deterministic version of the problem, a similar approach can be applied to check the feasibility of each neighbor in $O(1)$ time at the cost of maintaining, for each customer, the total demand served by the corresponding route up to that point, which is updated in linear time upon every change in the incumbent solution. The techniques present here allow one to check the feasibility of neighbor solutions exactly in $O(s)$ time for \mathcal{D}^{part} , and approximately in $O(1)$ time for \mathcal{D}^{card} , also at the cost of updating data structures whenever the incumbent solution is replaced. In the latter case, the time required by such updates is linear on the route length, but experiments below show that the proposed technique substantially reduces the overall algorithm run time by avoiding many exact tests. Moreover, as pointed out in Vidal et al. (2014), any local-search move composed of a bounded number of edge exchanges and node relocations can also be viewed as a recombination of a bounded number of subroutes from an incumbent solution. Thus, the new techniques may also be useful to improve the efficiency of other local search procedures that may be proposed for this problem.

Consider a robust CVRP solution containing two routes $r = (i_1, \dots, i_p, i_{p+1}, \dots, i_{|r|})$, and $r' = (j_1, \dots, j_q, j_{q+1}, \dots, j_{|r'|})$, each one defined by the sequence of customers they visit. A 2-OPT* move consists of either exchanging $(i_{p+1}, \dots, i_{|r|})$ with $(j_{q+1}, \dots, j_{|r'|})$ or exchanging $(i_{p+1}, \dots, i_{|r|})$ with (j_1, \dots, j_q) and then reversing both subroutes. Moreover, an *insert* move of i_{p+1} into r' can be viewed as two successive 2-OPT* moves: one exchanging $(i_{p+1}, \dots, i_{|r|})$ with $(j_{q+1}, \dots, j_{|r'|})$, and another exchanging $(j_{q+1}, \dots, j_{|r'|})$ with $(i_{p+2}, \dots, i_{|r|})$. Hence, we describe

the proposed feasibility test only for the route $r'' = (i_1, \dots, i_p, j_{q+1}, \dots, j_{|r''|})$, as it can be analogously used for the modified routes of all neighbors of a given solution containing r and r' , using the fact that subroute reversions do not affect the route feasibility.

For each $i \in V^0$, let $R(i)$ be the set of customers served by the only route that visits customer i in the current incumbent solution, until this visit (and including it). For example, considering the previously defined route r , $R(i_p) = \{i_1, \dots, i_p\}$. Let also $\bar{\Delta}(i) = \sum_{j \in R(i)} \bar{d}_j$. If the current

incumbent solution includes r and r' , $\bar{d}(r'') = \sum_{\ell=1}^p \bar{d}_{i_\ell} + \sum_{\ell=q+1}^{|r''|} \bar{d}_{j_\ell}$ can be computed in $O(1)$ time as $\bar{\Delta}(i_p) + \bar{\Delta}(j_{|r''|}) - \bar{\Delta}(j_q)$.

For \mathcal{D}^{part} , we propose to maintain also the value $\hat{\Delta}_k(i) = \sum_{j \in R(i) \cap V_k} \hat{d}_j$, for $k = 1, \dots, s$. In this case, the feasibility of r'' can be tested in $O(s)$ time by checking whether

$$\bar{d}(r'') + \min \left\{ b_k, \sum_{k=1}^s (\hat{\Delta}_k(i_p) + \hat{\Delta}_k(j_{|r''|}) - \hat{\Delta}_k(j_q)) \right\} \leq C.$$

Then, if r'' becomes a part of the incumbent solution, matrix $\hat{\Delta}$ can be updated in $O(s + |r''|)$ time.

For \mathcal{D}^{card} , the proposed technique uses the values $\hat{\Delta}(i) = \sum_{j \in R(i)} \hat{d}_j \xi_j^*$, and $\Lambda(i) = \sum_{j \in R(i)} \xi_j^*$, where ξ^* represents the worst case scenario for the current incumbent solution. For example, considering route r , ξ^* should maximize $\sum_{\ell=1}^{|r|} \hat{d}_{i_\ell} \xi_{i_\ell}$, subject to $\sum_{\ell=1}^{|r|} \xi_{i_\ell} \leq \Gamma$, and $\xi_{i_\ell} \in [0, 1]$, for $\ell = 1, \dots, |r|$. In this case, the feasibility of r'' can be approximately tested in $O(1)$ time by checking whether $\bar{d}(r'') + \tilde{d}(r'') \leq C$, where

$$\tilde{d}(r'') = \begin{cases} \tilde{d}_1 \Gamma_1 + \tilde{d}_2 \Gamma_2 & \text{if } \Gamma_1 + \Gamma_2 \leq \Gamma, \\ \tilde{d}_1 \Gamma_1 + \tilde{d}_2 (\Gamma - \Gamma_1) & \text{if } \Gamma_1 + \Gamma_2 > \Gamma \text{ and } \tilde{d}_1 \geq \tilde{d}_2, \\ \tilde{d}_1 (\Gamma - \Gamma_2) + \tilde{d}_2 \Gamma_2 & \text{if } \Gamma_1 + \Gamma_2 > \Gamma \text{ and } \tilde{d}_1 < \tilde{d}_2, \end{cases}$$

where $\Gamma_1 = \Lambda(i_p)$, $\Gamma_2 = \Lambda(j_{|r''|}) - \Lambda(j_q)$, $\tilde{d}_1 = \frac{\hat{\Delta}(i_p)}{\Gamma_1}$, and $\tilde{d}_2 = \frac{\hat{\Delta}(j_{|r''|}) - \hat{\Delta}(j_q)}{\Gamma_2}$. Note that Γ_1 and Γ_2 are the number of deviated demands in the subroutes (i_1, \dots, i_p) and $(j_{q+1}, \dots, j_{|r''|})$, respectively, and that \tilde{d}_1 and \tilde{d}_2 represent the average demand deviations in the same two subroutes. Later, we prove that r'' is necessarily infeasible if it does not pass in the proposed test. If r'' passes it, a full test must be performed. Vectors $\hat{\Delta}$ and Λ can be updated in $O(|r''|)$ time. For that, the true worst-case scenario for r'' must be calculated using a $O(|r''|)$ -time selection algorithm to find the Γ th largest demand deviation in r'' . In the experiments reported in Section 6, however, we use an $O(|r''| \log |r''|)$ implementation that sorts the demand deviations since the routes are typically not long enough to justify using a more specialized algorithm.

The next proposition proves the validity of the proposed feasibility test; its proof is deferred

to Section Appendix A.5 of the appendix.

Proposition 2. Let $\Xi = \left\{ \xi \in [0, 1]^n \mid \sum_{\ell=1}^p \xi_{i_\ell} + \sum_{\ell=q+1}^{|r'|} \xi_{j_\ell} \leq \Gamma \right\}$, and $\hat{d}(r'') = \max_{\xi \in \Xi} \left\{ \sum_{\ell=1}^p \hat{d}_{i_\ell} \xi_{i_\ell} + \sum_{\ell=q+1}^{|r'|} \hat{d}_{j_\ell} \xi_{j_\ell} \right\}$. Then, $\tilde{d}(r'') \leq \hat{d}(r'')$.

5.2. Iterated local search

Our ILS-VNS uses the four previously mentioned neighborhoods to improve the current solution. For each neighborhood, $O(n^2)$ possible neighbor solutions are evaluated at each iteration using the previously described data structures. For the inter-route neighborhoods the routes are searched in a random order that is updated upon each reached local optimum.

Each iteration of the main heuristic algorithm consists of two phases. In the first phase, a random single-route solution is generated and improved until reaching a local optimum with respect to a modified transportation cost $\tilde{c}_{ij} = \max \left\{ 0, \sqrt{c_{ij}^2 - 0.5(c_{0i} - c_{0j})^2} \right\}$ for each edge (i, j) . The expression used for \tilde{c}_{ij} aims to reduce the penalty for moving towards the depot. Then, this route is split into m non-empty subpaths. Each subpath is derived from the original route by taking from it the maximum number of consecutive vertices that fits into the vehicle capacity, starting from the first unvisited customer, and stopping when it remains as many vertices as the number of unused vehicles. If the obtained subpaths do not cover all customers, this initial solution is discarded and a new iteration is started. At most 100 iterations are performed trying to find a feasible solution. In the last iteration, however, the feasibility problem for the considered instance (packing all customers into m vehicles ignoring the transportation cost) is assumed to be hard enough for a special treatment. In this case, the well-known first-fit decreasing heuristic for the bin packing problem is used to pack the customers into vehicles, considering customers in a non-increasing order of their sum of mean and deviation demands. For every feasible solution found, the algorithm starts phase two to try to improve it. In this phase, each current solution is improved until reaching a local optimum with respect to the four neighborhoods previously mentioned. To escape from local optima, perturbations consisting of 3 customer exchanges between routes are applied. After each perturbation, the obtained solution is improved until reaching a local optimum. If the combination of perturbation and improvement does not lead to a smaller cost, the original solution is restored. Infeasible solutions that result from perturbations are discarded. The iteration finishes when no improvement is obtained after α perturbations are applied, where α is set to 1000 or 200, depending on whether the current solution cost is at most 2% greater than the best solution cost obtained so far or not.

Additional mechanisms are implemented to further speed-up the search over inter-route neighborhoods. These mechanisms are described in Section Appendix C.2 of the appendix.

6. Computational experiments

Extensive experiments have been performed to compare the proposed approach against the best known algorithms from the literature and to measure the impact of the proposed techniques over this algorithm. For \mathcal{D}^{part} , we used the 90 literature instances derived from the classical CVRP benchmark. For \mathcal{D}^{card} , we propose new instances. All experiments have run in an Intel(R) Core(TM) i7-3770 machine with 3.4 GHz and 12 gigabytes of RAM, using a single core.

6.1. Experiments for \mathcal{D}^{part}

The instances used to test the proposed algorithms for \mathcal{D}^{part} have been proposed by Gounaris et al. (2013) based on 90 classical CVRP instances ranging from 15 to 150 customers. Each deterministic instance has been used to generate one robust CVRP instance as follows:

- mean demands and deviations are equal to the nominal values multiplied by 0.9 and 0.2, respectively;
- vehicle capacities are increased by a factor of 1.2 with respect to the original ones;
- four partitions are created, each one corresponding to the set of customers positioned in one of the four quadrants of the customer area;
- the maximum sum of deviations allowed for each partition is computed as the sum of demand deviations of all customers in the corresponding quadrant multiplied by 0.75.

6.1.1. Heuristic performance

In this subsection, we compare our ILS-VNS heuristic against the AMP heuristic proposed by Gounaris et al. (2016) and the combination of this heuristic with the branch-and-cut algorithm proposed by Gounaris et al. (2013) (AMP+BC). For the ILS-VNS heuristic, we measure for each instance the gap between the cost of the best solution found in a first run after 100 iterations and the best known solution cost. All best known solutions are proved to be optimal except for the instance F-n135-k7. We also measure the average, best and worst time required to find a solution at least as good as in the first run over 10 runs. For comparison, we report averages of the results available in the literature for both AMP and AMP+BC which correspond to experiments run in an Intel 2.66 GHz processor with 3 GB RAM. The solution costs obtained by AMP are the best ones after 1 hour (3,600 seconds) of execution, and, for AMP+BC, are the best ones after running AMP for 5 minutes (300 seconds), and then BC for for 24 hours (86,400 seconds). For the instances that could be solved by BC, we used only the BC time reported in Gounaris et al. (2013). We also point out that considering 1 hour of runtime for AMP may be overestimated as the authors report that their results do not change much after the first 5 minutes. The overall results are summarized in Table 1. In this table, besides the headers, each row reports average results for one of the six instance classes of the corresponding classical CVRP benchmark. The last

row reports averages over all instances. Tables 2, and E.5,E.6, E.7 from the appendix follow the same row structure. For all these tables, the first two columns show respectively the instance class and the number of considered instances. For Table 1, the following three rows show the average solution cost gaps for ILS-VNS, AMP, and AMP+BC, respectively, each gap being followed by the number of optimal solutions between parenthesis. The remaining four columns report the geometric means of the three time measures (in seconds) taken for ILS-VNS and the runtimes of AMP+BC, respectively. Geometric means are preferred for all runtimes aggregated over different instances because many runtimes have different orders of magnitude.

Table 1: ILS-VNS heuristic results for \mathcal{D}^{part}

In. cls	# in.	GAP (#opt.)			ILS-VNS			AMP+BC t.
		ILS-VNS	AMP	AMP+BC	avg t.	min t.	max t.	
A	26	0.0531% (23)	0.3037% (17)	0.0218% (25)	1.51	0.67	2.76	3440.31
B	23	0.0000% (23)	0.0972% (18)	0.0289% (22)	1.15	0.62	1.78	250.96
E	11	0.0000% (11)	0.6254% (5)	0.0000% (11)	1.78	0.86	3.01	573.01
F	3	0.0000% (2)	0.6610% (1)	0.2080% (2)	5.84	3.44	10.37	55.76
M	3	0.0677% (2)	0.7104% (1)	0.2707% (2)	26.53	6.82	47.21	40681.81
P	24	0.0000% (23)	0.2122% (14)	0.0000% (23)	0.86	0.48	1.45	976.36
all	90	0.0176% (84)	0.2913% (56)	0.0296% (85)	1.42	0.71	2.41	981.90

By Table 1, it is clear that ILS-VNS significantly outperforms both AMP and AMP-BC even considering a runtime of 5 minutes (300 seconds) for AMP. ILS-VNS largely improves the solution quality with respect to AMP for all instance classes, in a time that is orders of magnitude smaller. The average gap improvement with respect to AMP+BC is smaller but still significant, except for the instance class A, where it is slightly worse. In this case, however, the difference between the runtimes of the two methods is even larger in most cases. Moreover, ILS-VNS found optimal solutions for all but 6 instances, only one less than the exact method AMP+BC, while AMP found such solution for a little more than half of the instances.

6.1.2. branch-and-cut-and-price performance

We also report in Table 2 consolidated results of the proposed branch-cut-and price method (BCP) and its comparison against AMP+BC. This table contains five columns reporting statistical data of the BCP root node, followed by three columns regarding the complete BCP runs and other three columns about AMP+BC. The BCP root columns report the average gaps between the pure columns generation lower bounds and the best know solution costs (gap 0), the mean runtime to obtain such bounds (t. 0), the average number of applied cut rounds (#c.r.), the average gaps between the final root node lower bounds and the best know solution costs (gap 1), and the mean runtime to obtain such bounds (t. 1). For both BCP and AMP+BC, the corresponding last two columns report the mean total runtime (t.) and the number of instances for which the solution optimality has been proved (#opt). For both methods, a runtime of 86,700 seconds is used when the instance cannot be solved within this time. Moreover, for BCP, the first column

gives the average number of branch-and-cut-and-price nodes ($\#n.$), and for AMP-BC, the first column gives the final gap between the obtained lower bound and the best known solution cost (gap).

Table 2: branch-and-cut-and-price results for \mathcal{D}^{part}

In. cls	# in.	BCP root					BCP			AMP+BC		
		gap 0	t. 0	#c.r.	gap 1	t. 1	#n.	t.	#opt.	gap	t.	#opt.
A	26	2.16%	0.70	3.7	0.00%	2.91	1.00	2.91	26	1.97%	3440.31	12
B	23	3.68%	1.31	2.8	0.01%	5.95	1.05	5.98	23	1.39%	250.96	13
E	11	2.31%	2.79	5.4	0.00%	11.40	1.00	11.40	11	2.19%	573.01	5
F	3	3.01%	139.10	5.0	0.30%	309.40	5.37	833.42	2	1.10%	55.76	2
M	3	1.66%	12.49	14.7	0.20%	52.44	3.33	153.51	3	2.70%	40681.81	1
P	24	1.27%	0.51	2.8	0.00%	1.47	1.00	1.48	24	2.09%	976.36	10
all	90	2.34%	1.17	3.9	0.02%	4.43	1.11	4.75	89	1.87%	981.90	43

By Table 2, it can be seen that the proposed BCP outperforms AMP+BC for all instance classes except F, where both methods solve two out of three instances having 44, 71 and 134 customers. In this case, the two smaller instances are harder for BCP because they have relatively long routes. Overall, BCP solves all instances but one while less than half of them are solved by AMP+BC. Although the only open instance has been tried for more than 24 hours without success, all other instances have been solved in less than 2 hours (7,200 seconds). Note that the mean runtime of BCP is two orders of magnitude smaller than that of AMP+BC. It is worth to mention that BCP used the solution cost found by ILS-VNS as an initial upper bound (we have used an upper bound one unit larger for all instances with up to 120 customers for testing purposes). However, it can be seen in Table 1 that adding the heuristic time to the total BCP time would not change much the results. It is also remarkable from Table 2 that the cuts closed almost all the gap left by the column generation lower bound, which allows us to solve almost all instances at the root node. Note however that the root node for BCP includes the resolution of IP problems generated through the enumeration of all useful elementary routes by CPLEX, when such problems are small enough. Nevertheless, the root lower bound used to compute the numbers in the column gap 1 does not include this resolution step.

6.1.3. Preprocessing

Applying the pre-processing detailed in Section 2.3, we could remove nearly 80% of the sub-problems, and 22 of 90 instances were reduced to deterministic homogeneous CVRP (with one subproblem). Further details are provided in Section Appendix E.1.1 of the appendix.

6.1.4. New capacity cuts

The literature cuts are already very effective, closing more than 60% of the gap. Yet, the new cuts close 33% of the remaining gap, which is a significant improvement. We refer to Section Appendix E.2 of the appendix for details.

6.2. Experiments for \mathcal{D}^{card}

6.2.1. New Instances

The new instances are also derived from the classical CVRP instances. As the uncertainty set \mathcal{D}^{card} makes the problem harder, the considered 90 instances ranges from 12 to 120 customers (we included the instances E-n13-k4 and A-n45-k7 not present in the \mathcal{D}^{part} data set and removed the largest F-n135-k7 and M-n151-k12). The additional data required to the robust counterpart has been generated based on the following three parameters: μ is the relative magnitude of demand deviations, ρ is the multiplicative factor applied to the average route length to compute the value of Γ , and τ is proportional to the difference between the vehicle capacity and the minimum required to make the instance feasible, where the scale factor applied makes τ equal to one if the capacity is the minimum required to use $m - 1$ vehicles. Smaller values of τ lead to tighter capacities. Further details on the generation of the specific robust counterpart parameters are given in Section Appendix D to ensure the reproducibility of results. We generated one main configuration and six additional ones to evaluate the sensitivity of results with respect to each instance parameters. Table 3 shows the assigned name (first row), and the value set to each parameter (remaining three rows) for each configuration. For example, in the main configuration, each demand deviation value is equal to 30% of the corresponding mean demand value, Γ is (approximately) equal to 75% of the average route length, and the difference between the vehicle capacity and its minimum is 30% of the difference between the capacity required to discard one vehicle and the minimum capacity.

Table 3: New benchmark set for \mathcal{D}^{card}

Conf.	Main	Low \hat{d}	High \hat{d}	Low Γ	High Γ	Low C	High C
μ	0.3	0.1	0.5	0.3	0.3	0.3	0.3
ρ	0.75	0.75	0.75	0.5	1	0.75	0.75
τ	0.3	0.3	0.3	0.3	0.3	0.15	0.6

6.2.2. Heuristic and branch-and-cut-and-price performance

Table 4 summarizes the results of running both ILS-VNS and BCP for the new benchmark instances. The ILS-VNS runs follow the same scheme as the one described in Subsection 6.1.1, and each BCP run was limited to 2 hours (7,200 seconds). In Table 4, the eight columns labeled by BCP root and BCP follow the same structure as in Table 2, and the last five columns report for ILS-VNS, the average gap (gap), the mean values for the average, minimum and maximum runtimes (avg t., min t., and max t.), and the number of optimal solutions found (#opt.), respectively. These values were computed in the same way as in Table 1.

Table 4: Heuristic and branch-and-cut-and-price results for \mathcal{D}^{card}

In. cls	# in.	BCP root					BCP			ILS-VNS				
		gap 0	t. 0	#c.	gap 1	t. 1	#n.	t.	#opt.	gap	avg t.	min t.	max t.	#opt.
A	27	2.19%	2.50	4.4	0.02%	17.88	1.11	18.81	27	0.03%	1.98	0.76	4.14	24
B	23	5.14%	3.44	5.9	0.23%	41.48	1.50	69.54	20	0.00%	2.57	1.01	5.04	19
E	13	1.91%	5.69	5.3	0.03%	24.84	1.16	27.79	13	0.12%	2.85	1.07	4.97	10
F	2	2.00%	154.53	0.5	0.00%	222.81	1.00	222.83	2	0.00%	1.26	1.20	1.33	2
M	2	4.03%	39.31	6.5	0.00%	108.21	1.00	108.23	2	0.00%	5.72	2.87	10.53	2
P	23	1.59%	2.28	3.4	0.00%	10.74	1.00	10.75	23	0.00%	1.93	0.74	3.85	23
all	90	2.79%	3.48	4.6	0.07%	22.47	1.17	26.47	87	0.03%	2.25	0.89	4.37	80
Low \hat{d}	90	2.79%	3.80	4.3	0.03%	26.14	1.13	28.60	89	0.00%	2.37	0.82	4.67	87
High \hat{d}	90	2.68%	3.36	4.9	0.16%	19.69	1.35	25.84	86	0.02%	3.50	0.94	7.14	82
Low Γ	90	2.74%	4.28	5.4	0.10%	27.71	1.20	30.97	89	0.01%	2.99	1.04	5.65	81
High Γ	90	2.67%	2.66	4.6	0.07%	14.77	1.17	17.20	87	0.02%	2.53	0.86	5.02	81
Low C	90	3.10%	3.79	6.5	0.43%	26.89	1.37	34.40	85	0.13%	6.10	1.46	13.58	69
High C	90	2.92%	3.83	4.6	0.18%	23.91	1.41	33.80	84	0.01%	1.95	0.85	3.35	80

By Table 4, it can be seen that the overall performance of the proposed methods for the new benchmark set is roughly similar to that observed for the literature instances: ILS-VNS can find the great majority of the optimal solutions in a few seconds, most of the gap left by the column generation lower bound is closed but the combination of the proposed cuts with the literature cuts previously proposed for the deterministic version, and only a few instances could not be solved exactly withing two hours of runtime. A more detailed analysis however reveals that there are some cases where instances can still be challenging for the proposed algorithms. For instance, ILS-VNS could not find optimal solutions for 21 out of 90 low-capacity instances and the average gap with respect to the best-known solutions is more than four times the gap of any other configuration. We observed that this is because it is harder to find feasible solutions with this configuration and the proposed method is not prepared to handle that. Moreover, for the main class, the three instances that could not be solved belong to the class B, having 50, 56 and 63 customers. It is worth mentioning that four larger instances of the same class could be solved relatively easily. The main reason for not solving such instances is that all of them have root gaps larger than 1.5%, which is more than 20 times larger than the average gap for the whole benchmark set in the main configuration. Regarding other configurations, it can be seen the instances with lower demand deviations are easier for both ILS-VNS and BCP in the sense that more optimal solutions are found by the heuristics, more instances could be solved exactly, and both the root gaps of BCP and the gaps of ILS-VNS with respect to the best known solution are smaller. We also observe that the root gaps of BCP are significantly larger for high demand deviations, and for both higher and lower capacities, in the latter case being more than six times larger than in the main configuration. For the lower capacity, we observed that the higher root gap is compensated by the stronger effect of fixing by reduced cost and enumeration in these instances, which leads to a number of solved instances than is not very much different from the main configuration. Overall, only 23 out of 630 instances could not be solved exactly within 2 hours, ranging from 50 to 100 customers, where 18 of them are from the class B, 4 are from the class E and 1 is from the class A.

6.2.3. Effect of approximate feasibility testing

We have also measured the effect of the proposed approximate feasibility checking procedure. For that, we measured the average runtime for each instance with this technique disable and enabled. The average ratio between the two times is 2.7 for the main configuration. For separate instance classes, this average ratio does not change much except for the classes F and M, which are 1.66 and 3.68, respectively. For more detailed results, we refer to Section Appendix E.3 on the appendix.

6.2.4. Preprocessing

The number of pricing problems left after the preprocessing is roughly 15% smaller than before, see Section Appendix E.1.2 of the appendix for details.

6.2.5. New capacity cuts

The literature cuts close 40% of the gap for these instances, and the new ones close nearly 40% of the remaining gap, see Section Appendix E.2 of the appendix.

7. Conclusion

Modern branch-and-cut-and-price algorithms have solved vehicle routing instances larger and faster than ever before. In this work, we carry over these techniques to the robust capacitated vehicle routing problems with knapsack uncertainty. Extending existing results in robust combinatorial optimization and providing original reduction strategies, new valid inequalities, and improved primal heuristics we are able to solve all but one instance proposed by Gounaris et al. (2013) for the partition polytope, while obtaining very good results for the new instances generated for the budget polytope.

Future work could seek to extend these good numerical results to other variants of robust vehicle routing problems, such as the one involving time windows and uncertain travel times. Yet, the later problem facing a strongly \mathcal{NP} -hard pricing problem in the robust case (Pessoa et al. 2015), its efficient solution would require more than a simple extension of the techniques presented in this work (however, if travel times are deterministic, the extension is straightforward). Further extensions could also apply the present decomposition approach to other combinatorial optimization problems with uncertainty in the binary knapsack substructure, such as the bin packing problem with item size uncertainty (Song et al. 2018).

References

- Aissi H, Bazgan C, Vanderpooten D (2009) Min-max and min-max regret versions of combinatorial optimization problems: A survey. *European Journal of Operational Research* 197(2):427–438.
- Álvarez-Miranda E, Ljubic I, Toth P (2013) A note on the bertsimas & sim algorithm for robust combinatorial optimization problems. *JOR* 11(4):349–360.
- Baldacci R, Christofides N, Mingozzi A (2008) An exact algorithm for the vehicle routing problem based on the set partitioning formulation with additional cuts. *Mathematical Programming* 115:351–385.
- Baldacci R, Mingozzi A, Roberti R (2011) New route relaxation and pricing strategies for the vehicle routing problem. *Operations Research* 59(5):1269–1283.
- Ben-Tal A, El Ghaoui L, Nemirovski A (2009) *Robust optimization* (Princeton University Press).
- Ben-Tal A, Goryashko AP, Guslitzer E, Nemirovski A (2004) Adjustable robust solutions of uncertain linear programs. *Math. Program.* 99(2):351–376.
- Ben-Tal A, Nemirovski A (1998) Robust convex optimization. *Math. Oper. Res.* 23(4):769–805.
- Bertsimas D, Sim M (2003) Robust discrete optimization and network flows. *Math. Program.* 98(1-3):49–71.
- Bertsimas D, Sim M (2004) The price of robustness. *Operations Research* 52(1):35–53.
- Birge JR, Louveaux FV (2011) *Introduction to Stochastic programming (2nd edition)* (Springer Verlag).

- Bulhoes T, Sadykov R, Uchoa E (2018) A branch-and-price algorithm for the minimum latency problem. *Computers & Operations Research* 93:66–78.
- Dinh T, Fukasawa R, Luedtke J (2018) Exact algorithms for the chance-constrained vehicle routing problem. *Mathematical Programming* In press.
- Fukasawa R, Longo H, Lysgaard J, Aragão MPd, Reis M, Uchoa E, Werneck RF (2006) Robust branch-and-cut-and-price for the capacitated vehicle routing problem. *Mathematical Programming* 106(3):491–511.
- Gendreau M, Laporte G, Séguin R (1996) Stochastic vehicle routing. *Eur. J. Oper. Res.* 88(1):3–12.
- Ghosal S, Wiesemann W (2018) The distributionally robust chance constrained vehicle routing problem. URL www.optimization-online.org/DB_HTML/2018/08/6759.html.
- Goetzmann K, Stiller S, Telha C (2011) Optimization over integers with robustness in cost and few constraints. *WAOA 2011, Saarbrücken, Germany, September 8-9, 2011, Revised Selected Papers*, 89–101.
- Gounaris CE, Repoussis PP, Tarantilis CD, Wiesemann W, Floudas CA (2016) An adaptive memory programming framework for the robust capacitated vehicle routing problem. *Transp. Sci.* 50(4):1239–1260.
- Gounaris CE, Wiesemann W, Floudas CA (2013) The robust capacitated vehicle routing problem under demand uncertainty. *Operations Research* 61(3):677–693.
- Irnich S, Desaulniers G (2005) *Shortest Path Problems with Resource Constraints*, 33–65 (Boston, MA: Springer US).
- Irnich S, Desaulniers G, Desrosiers J, Hadjar A (2010) Path-reduced costs for eliminating arcs in routing and scheduling. *INFORMS Journal on Computing* 22(2):297–313.
- Jepsen M, Petersen B, Spoorendonk S, Pisinger D (2008) Subset-row inequalities applied to the vehicle-routing problem with time windows. *Operations Research* 56(2):497–511.
- Kouvelis P, Yu G (2013) *Robust discrete optimization and its applications*, volume 14 (Springer Science & Business Media).
- Laporte G, Nohet Y (1983) A branch and bound algorithm for the capacitated vehicle routing problem. *Operations-Research-Spektrum* 5(2):77–85.
- Lee C, Lee K, Park K, Park S (2012) Technical note - branch-and-price-and-cut approach to the robust network design problem without flow bifurcations. *Operations Research* 60(3):604–610.
- Lee T, Kwon C (2014) A short note on the robust combinatorial optimization problems with cardinality constrained uncertainty. *4OR* 12(4):373–378.
- Lysgaard J, Letchford AN, Eglese RW (2004) A new branch-and-cut algorithm for the capacitated vehicle routing problem. *Mathematical Programming* 100(2):423–445.
- Ordóñez F (2010) Robust vehicle routing. *TUTORIALS in Operations Research* 153–178.
- Pecin D, Pessoa A, Poggi M, Uchoa E, Santos H (2017a) Limited memory rank-1 cuts for vehicle routing problems. *Operations Research Letters* 45(3):206 – 209.
- Pecin D, Pessoa AA, Poggi M, Uchoa E (2017b) Improved branch-cut-and-price for capacitated vehicle routing. *Math. Program. Comput.* 9(1):61–100.
- Penna PHV, Subramanian A, Ochi LS (2013) An iterated local search heuristic for the heterogeneous fleet vehicle routing problem. *Journal of Heuristics* 19(2):201–232.

- Pessoa A, Sadykov R, Uchoa E, Vanderbeck F (2018) Automation and combination of linear-programming based stabilization techniques in column generation. *INFORMS Journal on Computing* 30(2):339–360.
- Pessoa AA, Pugliese LDP, Guerriero F, Poss M (2015) Robust constrained shortest path problems under budgeted uncertainty. *Networks* 66(2):98–111.
- Poss M (2013) Robust combinatorial optimization with variable budgeted uncertainty. *4OR* 11(1):75–92.
- Poss M (2014) Robust combinatorial optimization with variable cost uncertainty. *EJOR* 237(3):836–845.
- Poss M (2018) Robust combinatorial optimization with knapsack uncertainty. *Dis. Opt.* 27:88–102.
- Righini G, Salani M (2006) Symmetry helps: Bounded bi-directional dynamic programming for the elementary shortest path problem with resource constraints. *Discrete Optimization* 3(3):255 – 273.
- Sadykov R, Uchoa E, Pessoa A (2017) A bucket graph based labeling algorithm with application to vehicle routing. Cadernos do LOGIS L-2017-7, UFF, URL <http://www2.logis.uff.br/cadernos/>.
- Song G, Kowalczyk D, Leus R (2018) The robust machine availability problem – bin packing under uncertainty. *IIE Transactions* In Press.
- Sungur I, Ordóñez F, Dessouky M (2008) A robust optimization approach for the capacitated vehicle routing. *IIE Transactions* 40(5):509–523.
- Tadayon B, Smith JC (2015) Algorithms and complexity analysis for robust single-machine scheduling problems. *J. Scheduling* 18(6):575–592.
- Talla Nobibon F, Leus R (2014) Complexity results and exact algorithms for robust knapsack problems. *J. Optim. Theory Appl.* 161(2):533–552.
- Uchoa E, Fukasawa R, Lysgaard J, Pessoa AA, de Aragão MP, Andrade D (2008) Robust branch-cut-and-price for the capacitated minimum spanning tree problem over a large extended formulation. *Math. Program.* 112(2):443–472, URL <http://dx.doi.org/10.1007/s10107-006-0043-y>.
- Vidal T, Crainic TG, Gendreau M, Prins C (2013) Heuristics for multi-attribute vehicle routing problems: A survey and synthesis. *European Journal of Operational Research* 231(1):1 – 21.
- Vidal T, Crainic TG, Gendreau M, Prins C (2014) A unified solution framework for multi-attribute vehicle routing problems. *European Journal of Operational Research* 234(3):658 – 673.
- Wiesemann W, Kuhn D, Sim M (2014) Distributionally robust convex optimization. *Oper. Res.* 62(6):1358–1376.

Appendix A. Missing proofs

Appendix A.1. Proof of Theorem 1

Let us first prove $\bigcup_{\theta \in \Theta} Y_{\theta}^{knap} \subseteq Y^{knap}$. Hence, let $y \in Y^{knap}$, and $\xi^* \in \arg\max_{\xi \in \Xi} \left\{ \sum_{i=1}^n \frac{\hat{d}_i}{w_i} \xi_i y_i \right\}$. By the strong duality of linear programming, we have that

$$b^{\top} \theta^* + (d^{\theta^*})^{\top} y = \bar{d}^{\top} y + b^{\top} \theta^* + w^{\top} z^* = \bar{d}^{\top} y + \sum_{i=1}^n \frac{\hat{d}_i}{w_i} \xi_i^* y_i \leq C,$$

where the last inequality holds because $y \in Y^{knap}$. Thus, $y \in Y_{\theta^*}^{knap}$.

To prove the reverse inclusion, let $y \in Y_{\theta'}^{knap}$ for some $\theta' \in \Theta$. We have that

$$\begin{aligned} \bar{d}^\top y + \max_{\xi \in \Xi} \left\{ \sum_{i=1}^n \frac{\hat{d}_i}{w_i} \xi_i y_i \right\} &= \\ \bar{d}^\top y + \min_{\theta \in \mathbb{R}_+^s} \left\{ b^\top \theta + \sum_{i=1}^n \max\{0, \hat{d}_i - w_i \theta_{k(i)}\} y_i \right\} &\leq \\ \bar{d}^\top y + b^\top \theta' + \sum_{i=1}^n \max\{0, \hat{d}_i - w_i \theta'_{k(i)}\} y_i &= \\ b^\top \theta' + (d^{\theta'})^\top y &\leq C. \end{aligned}$$

As a result, $y \in Y^{knap}$, finishing the proof.

Appendix A.2. Proof of Theorem 3

Clearly, $\bigcup_{\theta \in \Theta^*} \tilde{Y}_\theta^{knap} \subseteq \bigcup_{\theta \in \Theta^*} Y_\theta^{knap} = Y^{knap}$. Hence, we prove below that $Y^{knap} \subseteq \bigcup_{\theta \in \Theta^*} \tilde{Y}_\theta^{knap}$.

For that, let $y \in Y^{knap}$, and $\xi^* \in \operatorname{argmax}_{\xi \in \Xi} \left\{ \sum_{i=1}^n \frac{\hat{d}_i}{w_i} \xi_i y_i \right\}$. Assume also that ξ^* is an *extreme solution*, meaning that for all $i, j \in \{1, \dots, n\}$ with $i \neq j$, $\xi_i^*, \xi_j^* > 0$, and $k(i) = k(j)$, either $\xi_i^* = w_i$ or $\xi_j^* = w_j$. Note that a non-extreme solution may only be optimal if $\frac{\hat{d}_i}{w_i} y_i = \frac{\hat{d}_j}{w_j} y_j$ for all $i, j \in \{1, \dots, n\}$ with $i \neq j$, $\xi_i^*, \xi_j^* > 0$, $k(i) = k(j)$, $\xi_i^* < w_i$, and $\xi_j^* < w_j$. For each $k \in \{1, \dots, s\}$, let $I_k^* = \{i \in V_k \mid \xi_i^* > 0\}$, $\bar{I}_k^* = \{i \in V_k \mid \xi_i^* = w_i\}$. We further assume w.l.o.g. that $\xi_i^* > 0 \implies y_i = 1$ since letting $\xi_i^* > 0$ for some i with $y_i = 0$ does not help to increase the left-hand side of (2). Let also (θ^*, z^*) be an optimal solution to the left-hand side of (3), where the value of z_i^* is set as $\max\{0, \frac{\hat{d}_i}{w_i} y_i - \theta_{k(i)}^*\}$ for $i = 1, \dots, n$.

It remains to prove that y also satisfies

$$\sum_{\substack{i \in V_k \\ \hat{d}_i > w_i \theta_k^*}} w_i y_i \leq b_k \leq \sum_{\substack{i \in V_k \\ \hat{d}_i \geq w_i \theta_k^*}} w_i y_i, \quad \forall k \in \{1, \dots, s\} \mid \theta_k^* > 0, \quad (\text{A.1})$$

and

$$\sum_{i \in V_k} w_i y_i \leq b_k, \quad \forall k \in \{1, \dots, s\} \mid \theta_k^* = 0. \quad (\text{A.2})$$

For that, we use the complementary slackness of the solutions ξ^* and (θ^*, z^*) , as they are optimal to a linear programming problem and its dual, respectively. Namely, we have that

$$\theta_k^* > 0 \implies \sum_{i \in V_k} \xi_i^* = b_k,$$

for $k = 1, \dots, s$, and,

$$\xi_i^* > 0 \implies z_i^* + \theta_{k(i)}^* = \frac{\hat{d}_i}{w_i} y_i,$$

for $i = 1, \dots, n$. Given this fact, the second inequality of (A.1) holds because, since $\xi_i^* \leq w_i$ for all $i \in I_k^*$, and $\xi_i^* = 0$ for all $i \in I_k^* \setminus V_k$, we have that

$$b_k = \sum_{i \in V_k} \xi_i^* \leq \sum_{i \in I_k^*} w_i \leq \sum_{\substack{i \in V_k \\ \hat{d}_i \geq w_i \theta_k^*}} w_i y_i,$$

where the last inequality holds because both $\xi_i^* > 0$ and $z_i^* + \theta_{k(i)}^* = \frac{\hat{d}_i}{w_i} y_i$ together imply that $\hat{d}_i \geq w_i \theta_{k(i)}^*$. For the first inequality of (A.1), we have that

$$b_k = \sum_{i \in V_k} \xi_i^* \geq \sum_{i \in \bar{I}_k^*} w_i y_i \geq \sum_{\substack{i \in V_k \\ \hat{d}_i > w_i \theta_k^*}} w_i y_i,$$

where the first inequality holds by definition of I_k^* , and the second one is true because both $y_i = 1$ and $\hat{d}_i > w_i \theta_{k(i)}^*$ together imply that $z_i^* > 0$, which implies by complementary slackness between ξ_i^* and (θ^*, z^*) that $\xi_i^* = w_i$. Finally, (A.2) is also true because, since ξ^* is an optimal solution to the left-hand side of (2) and $\sum_{i \in V_k} \xi_i^* < b_k$, we have that $\xi_i^* = w_i$ for all $i \in V_k$ with $y_i = 1$ when $\theta_k^* = 0$.

Appendix A.3. Proof of Theorem 4

In order to be able to prove the theorem, we define a new optimization problem that turns out to be a relaxation of the problem of assigning the vertices of S to the minimum number of routes, respecting the vehicle capacities for demands in $\mathcal{D}^{part} = \{d = \bar{d} + \xi \mid \sum_{i \in V_k} \xi_i \leq b_k, k = 1, \dots, s, \xi \leq \kappa \bar{d}\}$. We call it the *Stripe Crossing Problem* (SCP).

In SCP, we are given s striped boards, where board k has height $q_k(S)$, for $k = 1, \dots, s$. Each board k has alternated gray and white horizontal stripes, the lowest one being gray. All gray stripes in board k have height $\frac{b_k}{\kappa}$, and all its white stripes have height $\max\{0, C - \frac{1+\kappa}{\kappa} b_k\}$, for $k = 1, \dots, s$. Only the highest stripe may have a truncated height if it does not fit into the remaining board space. Note that board k is completely gray if $C \leq \frac{1+\kappa}{\kappa} b_k$. SCP asks for a way to draw vertical lines crossing all stripes of all boards, from bottom to top, minimizing the number of used pens. It is assumed that each pen has a limited amount C of ink, and spends 1 and $1 + \kappa$ units of ink per line length unit in white and gray stripes, respectively. Moreover, each pen is allowed to draw at most one contiguous line segment in each board. Figure A.1 illustrates SCP by depicting an instance with 3 boards and a solution using 6 pens. The stripe heights of board 1 and the height of board 3 are indicated in the figure. Drawn lines are represented as wide dark-gray vertical lines with the corresponding pen indicated on the right.

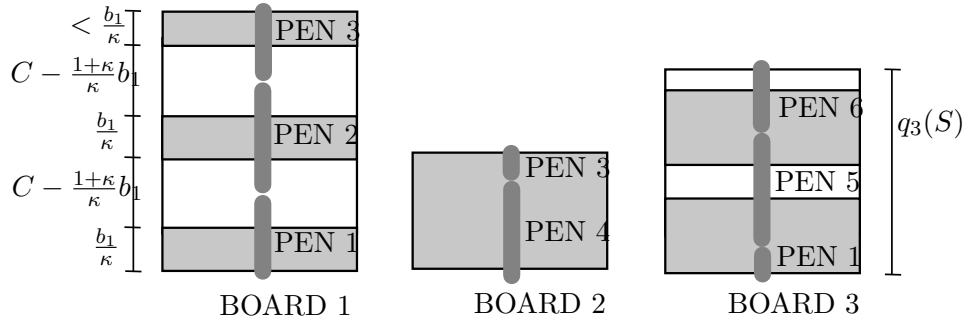


Figure A.1: A Stripe Crossing Problem instance.

Next, we present two propositions that demonstrate the link between SCP and the minimum number of vehicles required to serve all customers in a given set S . In this link, boards represent partitions, pens represent vehicles, gray stripes represent demands that deviate in a given scenario, and white stripes represent demands that do not deviate from their mean values. We also give an additional proposition proving that the newly proposed inequality strictly dominates (24).

Proposition 3. *The total line length drawn with a given pen over the gray stripes of a given board is at most $\frac{b_k}{\kappa}$.*

Proof. If $C \leq \frac{1+\kappa}{\kappa}b_k$, the proposition holds because the pen spends $1 + \kappa$ ink per length unit, being limited to a total length of $\frac{C}{1+\kappa} \leq \frac{b_k}{\kappa}$. Otherwise, suppose that a given pen draws a line length $\ell > \frac{b_k}{\kappa}$ over the gray stripes of a board k . Since the height of any gray stripe in this board is not greater than $\frac{b_k}{\kappa}$, the pen has to cross one of its white stripes completely. For that, it must spend at least $C - \frac{1+\kappa}{\kappa}b_k + (1 + \kappa)\ell > C$, which contradicts the limit on the amount of available ink for this pen, finishing the proof. \square

Proposition 4. *The optimal solution $r^*(S)$ of SCP is a lower bound on the number of routes required to serve all customers in S in the robust CVRP with the uncertainty set \mathcal{D}^{part} .*

Proof. Let y be a variable matrix representing a feasible solution for the robust CVRP with \mathcal{D}^{part} , where $y_{\ell i} = 1$ if vertex $i \in V^0$ is served by route $\ell \in \{1, \dots, m\}$, and 0 otherwise. We assume w.l.o.g. that routes $\ell = 1, \dots, r$, and only them, visit S . Then, it is enough to prove that there is a feasible solution to the corresponding SCP instance using r pens.

Associate each pen to a route ℓ , for $\ell = 1, \dots, r$. Then, for each board k , build a crossing vertical line by concatenating line segments drawn by all pens, such that the length of the line segment drawn by pen ℓ is given by $\sum_{i \in S \cap V_k} \bar{d}_i y_{\ell i}$. Note that the total line length drawn over the board k is given by $\sum_{\ell=1}^r \sum_{i \in S \cap V_k} \bar{d}_i y_{\ell i} = q_k(S)$ since all the demand of S is served by the r routes. Now, let $\alpha_{\ell k}$ and $\beta_{\ell k}$ be the total line length drawn by pen ℓ over the white and the gray stripes of board k , respectively, for $k = 1, \dots, s$, and $\ell = 1, \dots, r$. We have that the total ink spent by

each pen ℓ is given by

$$\begin{aligned}
\sum_{k=1}^s (\alpha_{\ell k} + (1 + \kappa)\beta_{\ell k}) &= \sum_{k=1}^s ((\alpha_{\ell k} + \beta_{\ell k}) + \kappa\beta_{\ell k}) \\
&\leq \sum_{k=1}^s \left(\sum_{i \in S \cap V_k} \bar{d}_i y_{\ell i} + \kappa \min \left\{ \frac{b_k}{\kappa}, \sum_{i \in S \cap V_k} \bar{d}_i y_{\ell i} \right\} \right) \\
&\leq \sum_{k=1}^s \left(\sum_{i \in V_k} \bar{d}_i y_{\ell i} + \min \left\{ b_k, \sum_{i \in V_k} \kappa \bar{d}_i y_{\ell i} \right\} \right) \\
&= \max_{d \in \mathcal{D}^{part}} \left\{ \sum_{i \in V^0} d_i y_{\ell i} \right\} \leq C
\end{aligned}$$

where the first inequality is a consequence of Proposition 3, and the last one holds because ℓ is a feasible route for the robust CVRP. Hence, the constructed solution is feasible for the SCP instance, finishing the proof. \square

We are now able to prove the main result of this section.

Proof. of Theorem 4

Proof. First, we show that γ_k is the exact line length drawn contiguously by a pen with ink C over the board k if it is used exclusively in this board. To see this, note that, for $C \leq \frac{1+\kappa}{\kappa}b_k$, where board k is completely gray, $\gamma_k = \frac{C}{1+\kappa}$ gives the exact length that can be drawn by a pen with ink C over a gray area. Otherwise, when $C > \frac{1+\kappa}{\kappa}b_k$, a pen with ink C spends $\frac{1+\kappa}{\kappa}b_k$ drawing a total length of $\frac{b_k}{\kappa}$ over the gray stripes, and the remaining ink to draw a total length of $C - \frac{1+\kappa}{\kappa}b_k$ over the white stripes. The sum of these lengths is exactly $\gamma_k = C - b_k$.

Now, note that $\left\lfloor \frac{q_k(S)}{\gamma_k} \right\rfloor$ is the number of times a pen becomes empty when crossing a board k (assuming that all pens used in this board are not used elsewhere). Moreover, $\hat{q}_k(S)$ is the remaining height of board k after excluding the part crossed by these pens. Given that, the exact total ink required to cross board k can be expressed as

$$C \left\lfloor \frac{q_k(S)}{\gamma_k} \right\rfloor + \hat{q}_k(S) + \kappa \min \left\{ \frac{b_k}{\kappa}, \hat{q}_k(S) \right\},$$

for $k = 1 \dots, s$. Thus, summing it up for all boards, dividing by C , and rounding the result up gives a lower bound on $r^*(S)$ which is exactly equal to $\hat{r}(S)$. Hence, by Proposition 4, $\hat{r}(S)$ is a valid lower bound on the left-hand side of (4) for any feasible robust CVRP solution. \square

Appendix A.4. Proof of Proposition 1

Note that, for the particular case considered here, $\tilde{r}(S)$ can be rewritten as

$$\left[\frac{\sum_{k=1}^s (q_k(S) + \min\{b_k, \kappa q_k(S)\})}{C} \right],$$

and

$$\begin{aligned} \dot{r}(S) &= \sum_{k=1}^s \sum_{i \in S \cap V_k} \min_{\theta \in \{0, e_k\}} \frac{d_i^\theta}{C - b^\top \theta} \\ &= \sum_{k=1}^s \sum_{i \in S \cap V_k} \min \left\{ \frac{(1 + \kappa) \bar{d}_i}{C}, \frac{\bar{d}_i}{C - b_k} \right\} \\ &= \sum_{k=1}^s \min \left\{ \frac{1 + \kappa}{C}, \frac{1}{C - b_k} \right\} q_k(S) \\ &= \sum_{k=1}^s \frac{1}{C} \left(q_k(S) + \min \left\{ \kappa, \frac{b_k}{C - b_k} \right\} q_k(S) \right), \end{aligned}$$

where e_k represents a vector with the k th component equal to one, and all remaining ones equal to zero. The first equality holds because the minimum of $\frac{d_i^\theta}{C - b^\top \theta}$ over $\tilde{\Theta}$ (here assumed to be equal to Θ) is always achieved when $\theta_\ell = 0$ for all $\ell \neq k$. Hence, to prove that $\hat{r}(S) \geq \max\{\lceil \dot{r}(S) \rceil, \tilde{r}(S)\}$, it is sufficient to show that

$$\begin{aligned} C \left\lfloor \frac{q_k(S)}{\gamma_k} \right\rfloor + \hat{q}_k(S) + \min\{b_k, \kappa \hat{q}_k(S)\} \\ \geq \max \left\{ q_k(S) + \min\{b_k, \kappa q_k(S)\}, q_k(S) + \min \left\{ \frac{b_k}{C - b_k}, \kappa \right\} q_k(S) \right\}, \end{aligned}$$

or, equivalently, that

$$C \left\lfloor \frac{q_k(S)}{\gamma_k} \right\rfloor + \hat{q}_k(S) + \min\{b_k, \kappa \hat{q}_k(S)\} \tag{A.3}$$

$$\geq q_k(S) + \min \left\{ \max \left\{ 1, \frac{q_k(S)}{C - b_k} \right\} b_k, \kappa q_k(S) \right\}, \tag{A.4}$$

for $k = 1, \dots, s$.

We divide into two cases. First, assume that $\frac{C}{1 + \kappa} \geq C - b_k$. This implies that

$$\gamma_k = \frac{C}{1 + \kappa}, \tag{A.5}$$

and also that $\frac{b_k}{\kappa} \geq \frac{C}{1 + \kappa} = \gamma_k$. Moreover, by definition of $\hat{q}_k(S)$, it is smaller than γ_k . Hence,

we have that

$$b_k > \kappa \hat{q}_k(S).$$

Applying this result, the definition of $\hat{q}_k(S)$, and (A.5) to (A.3) gives the expression

$$C \left\lfloor \frac{q_k(S)}{\gamma_k} \right\rfloor + (1 + \kappa) \left(q_k(S) - \frac{C}{1 + \kappa} \left\lfloor \frac{q_k(S)}{\gamma_k} \right\rfloor \right) = (1 + \kappa) q_k(S),$$

which is greater than or equal to (A.4).

Now, it remains to prove it for the case where $\frac{C}{1+\kappa} < C - b_k = \gamma_k$, which implies that

$$\begin{aligned} C &< (C - b_k) + \kappa \gamma_k \\ b_k &< \kappa \gamma_k. \end{aligned} \tag{A.6}$$

In this case, we may rewrite (A.3) as

$$\begin{aligned} C \left\lfloor \frac{q_k(S)}{\gamma_k} \right\rfloor + q_k(S) - (C - b_k) \left\lfloor \frac{q_k(S)}{\gamma_k} \right\rfloor + \min \left\{ b_k, \kappa q_k(S) - \kappa \gamma_k \left\lfloor \frac{q_k(S)}{\gamma_k} \right\rfloor \right\} \\ = q_k(S) + \min \left\{ \left(\left\lfloor \frac{q_k(S)}{\gamma_k} \right\rfloor + 1 \right) b_k, \kappa q_k(S) + (b_k - \kappa \gamma_k) \left\lfloor \frac{q_k(S)}{\gamma_k} \right\rfloor \right\}, \end{aligned}$$

which can be shown to be greater than or equal to (A.4) by applying (A.6).

To show that the inequality can be strict, we extend Example 3 by including the customers 5 and 6 in $S \cap V_2$, with $\bar{d}_5 = \bar{d}_6 = \hat{d}_5 = \bar{d}_6 = 2$. In this case, $\tilde{r}(S)$ remains equal to 2 because the deviation considered for partition 2 is already in its maximum, and the total demand to be served, including these deviations, increases from 7 to only $11 < 2C$. Moreover, $\dot{r}(S)$ increases by $\frac{d_5^{(0,1)}}{C-2} + \frac{d_6^{(0,1)}}{C-2} = 1$, becoming also equal to 2. However, $\hat{r}(S) = 3$ since $\gamma_2 = 4$, $q_2(S) = 8$, and $\hat{q}_1(S) = 1$.

Appendix A.5. Proof of Proposition 2

It is enough to prove that there exists $\xi \in \Xi$ such that $\sum_{\ell=1}^p \hat{d}_{i_\ell} \xi_{i_\ell} + \sum_{\ell=q+1}^{|r'|} \hat{d}_{j_\ell} \xi_{j_\ell} = \tilde{d}(r'')$. For that, we use the fact that ξ^* is the worst-case scenario for both r and r' . Clearly, if $\Gamma_1 + \Gamma_2 \leq \Gamma$ the proposition holds since $\tilde{d}(r'') = \sum_{\ell=1}^p \hat{d}_{i_\ell} \xi_{i_\ell}^* + \sum_{\ell=q+1}^{|r'|} \hat{d}_{j_\ell} \xi_{j_\ell}^*$. Next, we prove that it also holds only for $\Gamma_1 + \Gamma_2 > \Gamma$ and $\tilde{d}_1 \geq \tilde{d}_2$, since the remaining case is analogous. For that, let

$$\xi_\ell = \begin{cases} \frac{\Gamma - \Gamma_1}{\Gamma_2} \xi_\ell^* & \text{if } \ell \in \{j_{q+1}, \dots, j_{|r'|}\} \\ \xi_\ell^* & \text{otherwise.} \end{cases}$$

Clearly $\xi \in \Xi$. Moreover, since $\sum_{\ell=q+1}^{|r'|} \hat{d}_{j_\ell} \xi_{j_\ell} = (\Gamma - \Gamma_1) \sum_{\ell=q+1}^{|r'|} \frac{\hat{d}_{j_\ell} \xi_{j_\ell}^*}{\Gamma_2} = (\Gamma - \Gamma_1) \tilde{d}_2$, we have that

$$\sum_{\ell=1}^p \hat{d}_{i_\ell} \xi_{i_\ell} + \sum_{\ell=q+1}^{|r'|} \hat{d}_{j_\ell} \xi_{j_\ell} = \tilde{d}(r''), \text{ completing the proof.}$$

Appendix B. Three examples for the new capacity cuts

To simplify the cut strength analysis that follows, we assume from now on that $\tilde{\Theta} = \Theta$. The first two examples look at the case $\mathcal{D} = \mathcal{D}^{card}$.

Example 1. Consider that $S = \{1, \dots, 20\}$, $\Gamma = 1$, $C = 3$, and $\bar{d}_1 = \dots = \bar{d}_{20} = \hat{d}_1 = \dots = \hat{d}_{20} = 1$. In this case, since only one deviation is allowed for all $d \in \mathcal{D}$, we obtain that $\tilde{r}(S) = \lceil 21/3 \rceil = 7$. Alternatively, since $\tilde{\Theta} = \{0, 1\}$, we have that $\dot{r}(S) = 20 \min\{2/3, 1/2\} = 10$.

Although $\dot{r}(S)$ is usually much larger than $\tilde{r}(S)$ when the number of routes required to serve S is large, the next example shows that the opposite scenario may occur if only two routes are required.

Example 2. Consider $S = \{1, \dots, 5\}$, $\Gamma = 3$, $C = 15$, $\bar{d}_1 = \hat{d}_1 = 5$, and $\bar{d}_2 = \dots = \bar{d}_5 = \hat{d}_2 = \dots = \hat{d}_5 = 1$. In this case, since the total demand to be served in S can reach $16 > C$ (by deviating d_1 , d_2 , and d_3 , for example), we obtain that $\tilde{r}(S) = 2$. However, since $\tilde{\Theta} = \{0, 1\}$, we have that $\dot{r}(S) = \min\{10/15, 9/12\} + 4 \min\{2/15, 1/12\} = 1$.

Note that Example 1 can be easily adapted for $\mathcal{D} = \mathcal{D}^{part}$ because all deviations are unitary. For that, it is enough to assume that all customers in S belong to the same partition V_k of V^0 , and that $b_k = \Gamma = 1$. This shows that $\dot{r}(S)$ can also be strictly larger than $\tilde{r}(S)$ for the uncertainty set proposed in Gounaris et al. (2013). It is worth mentioning that all deviations in this example are proportional to the corresponding mean demand values, which is an assumption of the special case addressed by Theorem 4. The third example shows that the opposite strict inequality may also occur regardless of whether deviations are proportional to mean values or not.

Example 3. In this case, assume that V^0 is partitioned into two sets ($s = 2$), $S = \{1, 2, 3, 4\}$, and $S \cap V_1 = \{1\}$. Moreover, we have $C = 6$, $\bar{d}_1 = \dots = \bar{d}_4 = \hat{d}_1 = \dots = \hat{d}_4 = 1$, and $b_1 = b_2 = 2$. In this case, note that $\tilde{r}(S) = 2$ since the total deviation of d_2 , d_3 , and d_4 can reach the limit of the partition 2, and d_1 can deviate by one unity since it is in another partition, resulting in a total demand of $7 > C$ units to be served. However, since $\tilde{\Theta} = \{(0, 0), (0, 1), (1, 0), (1, 1)\}$, we have

$$\dot{r}(S) = \frac{d_1^{(1,0)}}{C-2} + \frac{d_2^{(0,1)}}{C-2} + \frac{d_3^{(0,1)}}{C-2} + \frac{d_4^{(0,1)}}{C-2} = 1.$$

Appendix C. Further algorithmic details

Appendix C.1. Separation of capacity cuts

Let \bar{x} be a fractional solution to RVRP-2IF. In our implementation, we separate robust capacity inequalities (24) at each node of the branch-and-bound tree using the heuristic described

in Algorithm 1, which is based on the separation heuristic used in Uchoa et al. (2008). In this algorithm, the limit on the number of inserted cuts is set to 500. Moreover, we use the procedure of Lysgaard et al. (2004) to separate the weaker version of (24) obtained by replacing its right-hand side with $\lceil \hat{r}(S) \rceil$. In this case, for each found violated cut, we insert the corresponding one from (24).

Algorithm 1: Separation heuristic for inequalities (24) or (4)

```

for  $i \in V^0$  do
   $S_i := \{i\}$ ;
  repeat
    Add to  $S_i$  the node  $j \in V^0 \setminus S_i$  that leads to the largest cut violation (or smallest
    slack) and results in a set not generated so far;
    Check if  $S_i$  leads to a violation;
    if the number of violated cuts found reaches the limit then
       $\perp$  return All violated cuts found
  until no such node  $j$  exists;
return All violated cuts found

```

Appendix C.2. Speeding-up the search over inter-route neighborhoods

In Algorithm 2, lines 2-5 implement the search in the two intra-route neighborhoods, where the incumbent solution is updated upon every found improvement. Inter-route neighborhoods are tried only after no more intra-route change can be made. Lines 7-21 and 22-31 implement the search in the 2-OPT* and the insert neighborhoods, respectively. For the 2-OPT*, since the change is symmetric, if the pair of routes (r, r') is tried in line 7, (r', r) is not tried. However, the pair $(r, \text{the reverse of } r')$ is also tried. In this case, the proposed mechanism to avoid trying useless changes uses the fact that, if a modified route is infeasible, the same route with one additional customer is still infeasible. This is done in lines 13 and 19 for route r , and lines 15 and 20 for route r' . A similar mechanism is implemented for the insert neighborhood, where an insertion that causes infeasibility will make the route infeasible regardless of the insertion position. This is implemented in lines 27 and 30, which avoid trying to insert the same customer in other positions in this case.

Appendix D. Instance generation

Here, we precisely describe the generation of the uncertainty set data for the new benchmark set proposed for \mathcal{D}^{card} . Given a deterministic CVRP instance and parameters μ , ρ and τ for a given configuration, the full specification of \mathcal{D}^{card} is computed as follows.

1. The mean demand vector \bar{d} is identical to the deterministic demand vector d of the original instance.

Algorithm 2: Local Search (parameter: an incumbent solution INC)

```

1 repeat
2   for each possible 2-OPT move over INC do
3     if it improves INC then replace INC by the new solution
4   for each possible reinsertion move over INC do
5     if it improves INC then replace INC by the new solution
6   if INC was not changed in the current iteration then
7     for each pair of routes  $r$  and  $r'$  in INC do
8       for  $p = 0, \dots, |r|$  do
9          $q_0 \leftarrow 0$ ;
10        for  $q = q_0, \dots, |r'|$  do
11          try exchanging the last  $|r| - p$  customers of  $r$  with the last  $|r'| - q$ 
12            customers of  $r'$ ;
13          if  $r$  fails in the approximate feasibility test then
14             $q_0 \leftarrow q + 1$ ; continue for;
15          if  $r'$  fails in the approximate feasibility test then
16            exit for;
17          if it improves the cost of INC then
18            if INC fails in the exact feasibility test then
19              if INC failed because of  $r$  then
20                 $q_0 \leftarrow q + 1$ ; continue for;
21              else exit for;
22            else replace INC by the new solution
23        for each pair of routes  $r$  and  $r'$  in INC do
24          for  $p = 1, \dots, |r|$  do
25            for  $q = 0, \dots, |r'|$  do
26              try inserting the  $p$ th customer of  $r$  after  $q$  customers in  $r'$ ;
27              if  $r'$  fails in the approximate feasibility test then
28                exit for;
29              if it improves the cost of INC then
30                if  $r'$  fails in the exact feasibility test then
31                  exit for;
32                else replace INC by the new solution
33 until INC does not change in the current iteration;

```

2. $\hat{d} = \mu\bar{d}$.

3. $\Gamma = \lfloor \frac{\rho n}{m} \rfloor$.

4. This last step is more involved since it aims to define a modified value for the vehicle capacity C ensuring that the resulting instance is feasible and the capacity is not too loose

(otherwise using a smaller number of vehicles would be desirable in practice). For that, we define a function $\text{BP}(c)$ that receives a tentative capacity value c and computes an upper approximation of the minimum number of vehicles required to make the current robust CVRP instance feasible with c as the vehicle capacity. The algorithm used to evaluate BP is detailed later. Then, we set $C = \tau C_{\min} + (1 - \tau) C_{\max}$, where $C_{\min} = \min\{c \in \mathbb{N} \mid \text{BP}(c) \leq m\}$ and $C_{\max} = \min\{c \in \mathbb{N} \mid \text{BP}(c) \leq m - 1\}$.

First, we remark that function $\text{BP}(c)$ can be fulfilled by any heuristic for the robust counterpart of the Bin Packing Problem (BPP). To see this, note that BP ignores the objective function of the robust CVRP instance being processed and tries to pack the customer into the minimum number of identical vehicles with capacity c . Thus, we compute BP using the well-known first-fit decreasing heuristic for the deterministic version of BPP, where customers are ordered in a non-increasing order by the sum of their maximum demands allowed by the uncertainty set. At each iteration, the heuristic searches in the ordered list of customers for the first one that fits into the current vehicle. Whenever no customers can be inserted in the current vehicle, a new vehicle is inserted in the solution. Although this method is not guaranteed to compute the minimum number of vehicles required, we observed that instances created with $\tau = 0$ were not realistic since their solution costs (now considering the CVRP objective function) usually increased by large factors with respect to the deterministic version of the problem. Thus, we decided restrict our attention to instances with $\tau \geq 1.5$. For the sake of easy reproducibility of our results, we report the values of C_{\min} and C_{\max} for all instances of the proposed benchmark set in Subsection Appendix F.1.

Appendix E. Detailed numerical experiments

Appendix E.1. Effect of preprocessing

Appendix E.1.1. Uncertainty set \mathcal{D}^{part}

Table E.5 shows the effect of the preprocessing technique introduced in Subsection 2.3 based in Corollary 2 for \mathcal{D}^{part} . In this table, the last 4 columns shows the average number of vehicles (m), the average number of subproblems after preprocessing ($\#sp$), the percentage reduction ($\%red.$) obtained with respect to the initial number of subproblems, which is always equal to $2^8 = 16$, and the number of instances that could be solved as deterministic CVRP because only one subproblem remained.

From Table E.5, it can be seen that the proposed preprocessing method is very effective for the literature instances. Almost 80% of the subproblems have been removed, and 22 of 90 instances were solved as deterministic CVRP. Moreover, the preprocessing method seems to be more effective for instance classes where the average number of vehicles is larger. We believe that this is not a coincidence and that the way instances have been generated favors the observed reduction. Recall that the limit on the total demand deviation for each quadrant is fixed as 75% of the sum

Table E.5: Effect of preprocessing for \mathcal{D}^{part}

In. cls	#in.	m	#sp	%red.	#det.
A	26	7.1	2.7	83.4%	7
B	23	7.2	3.9	75.8%	0
E	11	7.3	3.6	77.3%	4
F	3	5.0	5.0	68.8%	0
M	3	9.7	1.3	91.7%	2
P	24	7.3	4.3	73.2%	9
all	90	7.2	3.6	77.8%	22

of demand deviations. Since each quadrant has roughly 25% of the total demand to be served and deviations are proportional to mean demand values, the limit imposed to the total demand deviation can only be reached for a route the serves roughly 18.75% ($> 1/6$) of the total demand. Thus, if the number vehicles is much larger than 6, the preprocessing step is likely to prove that total deviation limit cannot be reached for many quadrants. This hypothesis is confirmed by the chart of Figure E.2, where each point represents one or more instances whose coordinates are the number of vehicles and the number of remaining subproblems after preprocessing. The decrease on the number of subproblems as the number of vehicles increases is very clear.

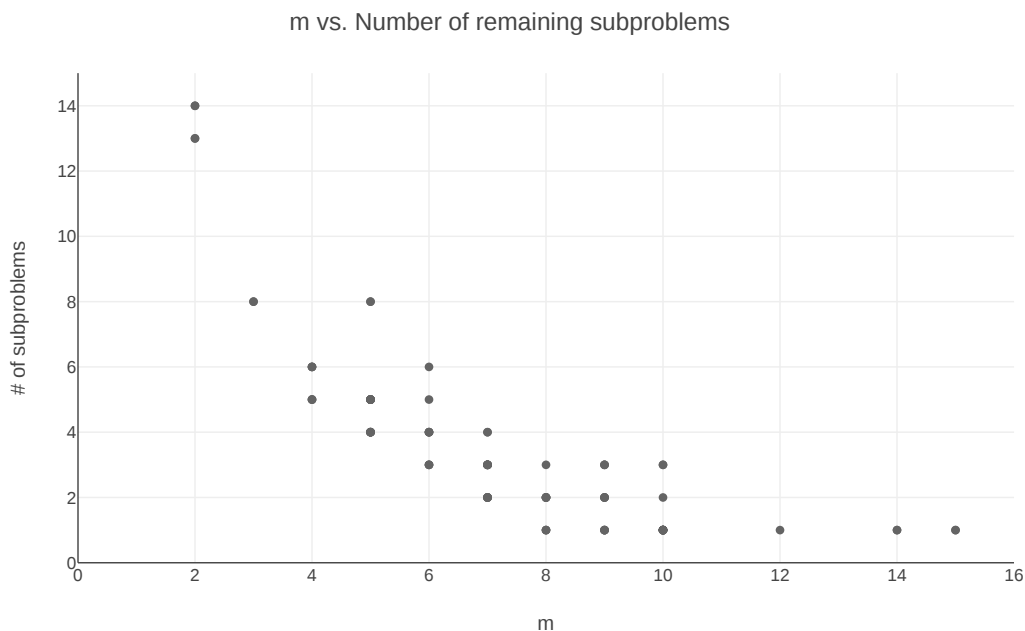


Figure E.2: Relation between the number of vehicles and the number of subproblems remaining after preprocessing.

Although the previous observation has been caused a specific artificial property of the benchmark set, we believe that similar situations may occur in real-life applications, leading to im-

pressive reductions on the number of subproblems. For testing robust optimization algorithms however, it is now desirable that the new benchmark sets are designed to avoid the existence of redundant constraints in the uncertainty set description. This is the case for the new benchmark set proposed in Subsection 6.2.1.

Appendix E.1.2. Uncertainty set \mathcal{D}^{card}

Table E.6 presents a measure of the effect of preprocessing the subproblems. In this table, the first seven rows after the headers refer to the main configuration described in the previous subsection, containing results for each instance class separately, and then aggregated results. The additional six rows provide aggregated results for all instance classes considering the remaining configurations. The results in these rows should be compared with that in the seventh row. The first two columns contain the instance class or configuration identifier (In. cls), and the number of instances in that subset (#in.). Tables 4, E.8, and E.7 following the same format except that results for configurations other than the main one are not presented in the last two tables. The last four columns of Table E.6 contain the average number of distinct demand values (#dem.), the average number of subproblems without preprocessing (#sp lit.) according to Theorem 2, and the average number of subproblems after preprocessing (#sp new), and the percentage reduction (%red.).

Table E.6: Effect of preprocessing for \mathcal{D}^{card}

In. cls	#in.	#dem.	#sp lit.	#sp new	%red.
A	27	20.7	16.6	13.7	16.7%
B	23	21.6	16.9	14.0	16.9%
E	13	24.3	17.4	14.1	16.0%
F	2	53.5	24.5	21.5	11.9%
M	2	14.0	10.5	8.5	26.3%
P	23	25.5	18.3	16.2	9.4%
all	90	22.7	17.0	14.4	14.7%
Low \hat{d}	90	22.7	17.0	14.8	12.4%
High \hat{d}	90	22.7	17.0	14.1	16.1%
Low Γ	90	22.7	17.8	17.7	0.8%
High Γ	90	22.7	16.1	10.6	32.6%
Low C	90	22.7	17.0	14.2	16.0%
High C	90	22.7	17.0	14.9	11.6%

From Table E.6, we observe that the effect of preprocessing is not so expressive but still significant for the new benchmark instances. This was expected since the instances have been generated in a way that Γ is never larger than the average route length. We also observe that the effect of preprocessing increases for larger values of Γ , and that Theorem 2 provides an important reduction on the number of subproblems with respect to the number of distinct demand values

but it is far away from dividing it by two because most instances have a large number of customers with the same associated demand.

Appendix E.2. Effect of new capacity cuts

The aim of this subsection is to present a measure of the effect of the strengthened robust capacity cuts introduced in Subsection 4 for the generic uncertainty set \mathcal{D}^{knep} , and its specific version given by Theorem 4 for \mathcal{D}^{part} assuming demand deviations proportional to the corresponding mean demand value. The results presented in this table were obtained in a run of BCP only for the root node, with all other cuts, fixing by reduced cost and enumeration of useful elementary routes disabled. We compare two runs. In the first one, only the capacity inequalities proposed by Gounaris et al. (2013) are separated using the procedure described in Section Appendix C.1 of the appendix. The second one separates the new cuts using both this procedure and the one proposed by Lysgaard et al. (2004) for the deterministic CVRP. In the second case, the separation algorithm receives modified demands described in Subsection 4, and the violated cuts found are replaced by the strongest available ones, which are the specific version for \mathcal{D}^{part} and the more generic version for \mathcal{D}^{card} . For \mathcal{D}^{card} , we considered only the main configuration.

Table E.7 presents the obtained results. In this table, the columns labeled by “#in” report the number of instances considered in each row, which is different for \mathcal{D}^{part} and \mathcal{D}^{card} . These numbers may be smaller than in the previous tables because we disregard all instance for which the gap left by the pure column generation lower bound is zero. The columns labeled by “cl. gap” and “gap rd.” show the averages of the percentage gap closed by the literature cuts and the percentage reduction of the gap obtained by replacing the literature cuts with the newly proposed strengthened cuts. Let 1stLB, litLB, and newLB be the root lower bounds obtained by BCP without any cut, without only literature cuts, and with the new cuts. Let also UB be the best known solution cost. The percentage gap closed by the literature cuts and the percentage gap reduction obtained with the new cuts are given by $\frac{\text{litLB}-\text{1stLB}}{\text{UB}-\text{1stLB}} \times 100\%$ and $\frac{\text{newLB}-\text{litLB}}{\text{UB}-\text{litLB}} \times 100\%$, respectively. Because of that, the instances for which the gap left by the literature cuts is zero are disregarded in the columns under the header “New cuts”. The remaining six columns show two additional measures for each run of each benchmark set: the number of closed instances, i.e. that with final gap zero, labeled by “#cl.”, and the average number of cut rounds needed, labeled by “#c.r.”.

Overall, Table E.7 shows that the literature cuts are very effective for \mathcal{D}^{part} as they close more than 60% of the gap, and that the new cuts close 33% of the remaining gap, which is a significant improvement. However, the performance of the new cuts is highly dependent on the instance class. For example, it closes almost 80% of the remaining gap for the class M and more than 50% for the classes B and F. Moreover, the number of instances with gap zero increases from 13 to 17 with the new cuts. It is also clear that a small number of cut rounds are required for convergence in both cases. For \mathcal{D}^{card} , we note that the gap zero is obtained for less instances (only 5 with the literature cuts and 6 with the new cuts), and the literature cuts are less effective in general,

Table E.7: Effect of the new capacity cuts

In. cls	# in.	\mathcal{D}^{part}						# in.	\mathcal{D}^{card}					
		Lit. cuts			New cuts				Lit. cuts			New cuts		
		cl. gap	#cl.	#c.r.	gap rd.	#cl.	#c.r.		cl. gap	#cl.	#c.r.	gap rd.	#cl.	#c.r.
A	25	55.9%	1	2.8	36.2%	0	2.9	27	33.4%	0	2.7	37.9%	0	2.9
B	23	81.4%	5	2.7	51.5%	8	2.8	23	53.3%	0	2.7	64.5%	0	2.9
E	11	45.7%	2	2.5	9.3%	2	2.5	13	38.2%	3	1.8	25.3%	4	2.2
F	2	91.6%	1	1.5	58.7%	1	2	2	43.5%	0	1	-14.6%	0	2
M	2	68.8%	0	2.5	77.6%	1	3	2	67.5%	0	3	27.2%	0	3
P	22	51.4%	4	2.3	17.6%	5	2.3	22	32.2%	2	2.1	17.6%	2	2.8
all	85	61.5%	13	2.6	33.5%	17	2.6	89	39.9%	5	2.4	37.3%	6	2.7

closing roughly 40% of the column generation gap only. From that gap, the new cuts close more than 37% in the average, again with a large variation from one instance class to the other. For example, for the class B, which is the hardest one for BCP, the gaps closed by both the literature cuts and the new cuts are much larger than for other classes. This suggests that further improving these cuts may be a way to solve the instances left open by this work. However, for the class F, the new cuts provided lower bounds that are worse in the average than that of the literature cuts. This is only possible because the cut separation routine used is not exact. In fact, this happened only for the instance F-n45-k4, where the literature cuts closed 87.1% of the initial gap and the new cuts closed only 81.4% of this initial gap, resulting in a gap 43.4% larger than the gap left by the literature cuts.

Appendix E.3. Effect of approximate feasibility checking for \mathcal{D}^{card}

Table E.8 compares the runtimes of ILS-VNS with and without performing approximate feasibility checks, for \mathcal{D}^{card} . The last three columns of this table contains the mean runtimes performing these checks (app.t.time), the mean runtimes not performing them, i.e. performing only exact checks (ex.t.time), and the average ratio between the time spent not performing the checks and the time spent performing them (ex.app.ratio).

Table E.8: Effect of the approximate feasibility testing for \mathcal{D}^{card}

In. cls	# in.	app.t. time	ex.t. time	ex.app. ratio
A	27	1.98	5.82	2.96
B	23	2.57	7.09	2.78
E	13	2.85	6.79	2.47
F	2	1.26	2.07	1.66
M	2	5.72	21.04	3.68
P	23	1.93	4.47	2.47
all	90	2.25	5.88	2.70

Appendix F. Raw data for Reproducibility*Appendix F.1. Capacity ranges for the new benchmark set*Table F.9: Minimum and maximum capacities for \mathcal{D}^{card}

Inst.	C_{min}	C_{min}	Inst.	C_{min}	C_{min}	Inst.	C_{min}	C_{min}
A-n32-k5	104	126	B-n38-k6	108	126	E-n76-k14	123	132
A-n33-k5	111	135	B-n39-k5	111	135	E-n101-k8	228	258
A-n33-k6	115	134	B-n41-k6	120	141	E-n101-k14	130	140
A-n34-k5	116	139	B-n43-k6	110	129	F-n45-k4	2275	3019
A-n36-k5	112	137	B-n44-k7	115	132	F-n72-k4	36382	48097
A-n37-k5	104	128	B-n45-k5	124	151	M-n101-k10	231	251
A-n37-k6	119	140	B-n45-k6	124	146	M-n121-k7	244	280
A-n38-k5	121	148	B-n50-k7	110	127	P-n19-k2	194	358
A-n39-k5	121	148	B-n50-k8	116	129	P-n20-k2	196	363
A-n39-k6	110	129	B-n51-k7	123	141	P-n21-k2	186	347
A-n44-k6	120	141	B-n52-k7	109	125	P-n22-k2	193	357
A-n45-k6	125	147	B-n56-k7	110	126	P-n22-k8	3420	3790
A-n45-k7	114	129	B-n57-k7	127	145	P-n23-k8	50	57
A-n46-k7	108	123	B-n57-k9	112	124	P-n40-k5	155	188
A-n48-k7	114	130	B-n63-k10	116	127	P-n45-k5	173	210
A-n53-k7	121	140	B-n64-k9	124	137	P-n50-k7	170	195
A-n54-k7	121	138	B-n66-k9	121	134	P-n50-k8	148	166
A-n55-k9	116	129	B-n67-k10	114	124	P-n50-k10	117	128
A-n60-k9	115	128	B-n68-k9	117	130	P-n51-k10	96	106
A-n61-k9	124	138	B-n78-k10	119	130	P-n55-k7	184	209
A-n62-k8	116	131	E-n13-k4	5820	7420	P-n55-k8	164	184
A-n63-k9	124	138	E-n22-k4	6940	9000	P-n55-k10	131	143
A-n63-k10	117	129	E-n23-k3	5330	6266	P-n55-k15	85	90
A-n64-k9	120	133	E-n30-k3	5330	7865	P-n60-k10	141	155
A-n65-k9	123	137	E-n31-k7	163	190	P-n60-k15	91	96
A-n69-k9	118	131	E-n33-k4	9260	12129	P-n65-k10	150	165
A-n80-k10	118	130	E-n51-k5	194	237	P-n70-k10	164	181
B-n31-k5	103	126	E-n76-k7	245	280	P-n76-k4	427	553
B-n34-k5	115	141	E-n76-k8	214	241	P-n76-k5	341	416
B-n35-k5	111	137	E-n76-k10	170	186	P-n101-k4	457	594

Appendix F.2. Raw ILS-VNS results for \mathcal{D}^{part}

Inst.	UB	avg t.	min t.	max t.	Inst.	UB	avg t.	min t.	max t.
A-n32-k5	748	0.30	0.30	0.31	B-n66-k9	1251	2.75	0.93	6.49
A-n33-k5	642	0.28	0.24	0.31	B-n67-k10	1007	1.15	1.04	1.61
A-n33-k6	717	0.30	0.26	0.55	B-n68-k9	1205	31.25	1.84	112.23
A-n34-k5	715	0.32	0.29	0.38	B-n78-k10	1131	6.57	1.29	20.89
A-n36-k5	755	0.40	0.30	0.64	E-n22-k4	373	0.14	0.14	0.14
A-n37-k5	650	0.41	0.37	0.45	E-n23-k3	563	0.29	0.22	0.52
A-n37-k6	892	0.31	0.30	0.33	E-n30-k3	475	0.29	0.28	0.29
A-n38-k5	704	1.20	0.40	3.84	E-n33-k4	814	0.37	0.37	0.37
A-n39-k5	777	0.64	0.37	1.36	E-n51-k5	516	0.84	0.81	0.88
A-n39-k6	787	0.40	0.38	0.49	E-n76-k7	661	4.20	1.56	8.87
A-n44-k6	909	2.35	0.60	4.32	E-n76-k8	709	7.30	1.43	13.69
A-n45-k6	896	2.50	1.42	4.52	E-n76-k10	796	42.78	5.95	173.49
A-n46-k7	888	0.62	0.53	1.04	E-n76-k14	952	1.78	0.93	3.50
A-n48-k7	1033	0.63	0.53	0.96	E-n101-k8	789	8.90	2.93	21.58
A-n53-k7	974	0.71	0.59	0.93	E-n101-k14	1011	7.40	1.98	16.40
A-n54-k7	1106	2.32	0.52	7.68	F-n45-k4	718	0.85	0.64	1.18
A-n55-k9	1030	3.68	1.49	8.98	F-n72-k4	232	2.10	2.04	2.20
A-n60-k9	1280	1.66	0.86	4.14	F-n135-k7	1122	112.18	30.99	428.40
A-n61-k9	983	87.32	1.74	309.07	M-n101-k10	809	2.97	2.84	3.34
A-n62-k8	1219	4.29	1.05	10.08	M-n121-k7	994	6.83	3.11	13.04
A-n63-k9	1505	7.75	1.66	14.44	M-n151-k12	987	921.55	35.81	2416.68
A-n63-k10	1244	3.34	1.36	7.73	P-n16-k8	439	0.05	0.05	0.05
A-n64-k9	1326	2.78	0.89	5.08	P-n19-k2	195	0.12	0.12	0.12
A-n65-k9	1106	4.85	1.28	13.12	P-n20-k2	208	0.15	0.15	0.15
A-n69-k9	1109	7.13	1.71	12.66	P-n21-k2	208	0.17	0.16	0.17
A-n80-k10	1662	16.17	3.48	38.97	P-n22-k2	213	0.17	0.17	0.17
B-n31-k5	651	0.25	0.24	0.28	P-n22-k8	537	0.09	0.09	0.09
B-n34-k5	768	0.31	0.30	0.31	P-n23-k8	504	0.14	0.09	0.30
B-n35-k5	883	0.31	0.26	0.37	P-n40-k5	447	0.60	0.41	1.15
B-n38-k6	729	0.39	0.38	0.39	P-n45-k5	501	0.64	0.60	0.67
B-n39-k5	532	0.42	0.39	0.52	P-n50-k7	539	2.43	0.59	7.15
B-n41-k6	796	0.39	0.35	0.50	P-n50-k8	592	0.60	0.45	0.97
B-n43-k6	681	0.49	0.47	0.52	P-n50-k10	656	0.58	0.43	0.90
B-n44-k7	835	0.37	0.35	0.38	P-n51-k10	707	1.58	0.82	2.98
B-n45-k5	701	0.56	0.55	0.58	P-n55-k7	549	2.27	0.74	5.54
B-n45-k6	660	0.51	0.44	0.89	P-n55-k8	572	1.24	0.69	2.67

B-n50-k7	679	0.73	0.66	0.97	P-n55-k10	670	1.59	0.60	2.56
B-n50-k8	1224	5.97	0.98	15.52	P-n55-k15	889	1.04	0.48	2.17
B-n51-k7	961	2.85	0.66	7.22	P-n60-k10	712	0.82	0.65	1.95
B-n52-k7	675	0.88	0.71	1.32	P-n60-k15	931	26.82	2.50	74.61
B-n56-k7	623	0.78	0.76	0.80	P-n65-k10	765	8.40	1.33	21.81
B-n57-k7	1055	0.86	0.67	1.27	P-n70-k10	785	2.59	0.71	6.69
B-n57-k9	1540	25.60	2.42	67.59	P-n76-k4	590	3.75	2.45	6.01
B-n63-k10	1407	3.05	0.60	7.17	P-n76-k5	616	3.64	1.94	8.64
B-n64-k9	803	0.93	0.90	0.99	P-n101-k4	673	5.43	4.60	7.08

Appendix F.3. Raw BCP results for \mathcal{D}^{part}

Inst.	root LB	UB	time	Inst.	root LB	UB	time
A-n32-k5	748.0	748	0.42	B-n66-k9	1249.2	1251	47.11
A-n33-k5	630.7	642	2.65	B-n67-k10	1006.0	1007	13.03
A-n33-k6	705.7	717	0.60	B-n68-k9	1204.1	1205	24.46
A-n34-k5	708.8	715	0.60	B-n78-k10	1130.3	1131	24.73
A-n36-k5	742.0	755	1.46	E-n22-k4	362.5	373	1.75
A-n37-k5	645.4	650	1.96	E-n23-k3	550.3	563	8.23
A-n37-k6	881.0	892	0.72	E-n30-k3	475.0	475	19.62
A-n38-k5	698.5	704	1.37	E-n33-k4	807.3	814	35.91
A-n39-k5	775.2	777	1.87	E-n51-k5	515.0	516	5.44
A-n39-k6	777.3	787	0.81	E-n76-k7	660.2	661	20.89
A-n44-k6	902.5	909	2.99	E-n76-k8	707.5	709	12.72
A-n45-k6	894.2	896	1.82	E-n76-k10	793.7	796	8.54
A-n46-k7	885.0	888	2.68	E-n76-k14	947.6	952	2.03
A-n48-k7	1026.4	1033	4.78	E-n101-k8	788.7	789	232.46
A-n53-k7	972.0	974	12.01	E-n101-k14	1011.0	1011	7.16
A-n54-k7	1105.5	1106	7.70	F-n45-k4	715.1	718	38.41
A-n55-k9	1023.8	1030	1.89	F-n72-k4	232.0	232	173.85
A-n60-k9	1276.2	1280	4.65	F-n135-k7	1111.8	<u>1122</u>	86700.00
A-n61-k9	978.4	983	5.28	M-n101-k10	806.3	809	3.18
A-n62-k8	1202.6	1214	15.46	M-n121-k7	993.4	994	163.50
A-n63-k9	1503.1	1505	4.79	M-n151-k12	979.1	985	6949.66
A-n63-k10	1233.0	1233	14.47	P-n16-k8	434.5	439	0.02
A-n64-k9	1321.8	1325	16.45	P-n19-k2	195.0	195	0.63
A-n65-k9	1101.8	1106	1.09	P-n20-k2	207.8	208	0.61
A-n69-k9	1105.5	1109	8.75	P-n21-k2	207.3	208	1.14
A-n80-k10	1659.1	1662	13.68	P-n22-k2	209.9	213	1.21

B-n31-k5	649.8	651	0.90	P-n22-k8	537.0	537	0.13
B-n34-k5	768.0	768	10.43	P-n23-k8	500.8	504	0.04
B-n35-k5	883.0	883	1.51	P-n40-k5	442.2	447	1.18
B-n38-k6	728.3	729	1.16	P-n45-k5	496.7	501	4.73
B-n39-k5	532.0	532	9.64	P-n50-k7	535.0	539	2.47
B-n41-k6	793.9	796	4.29	P-n50-k8	586.8	592	0.34
B-n43-k6	678.7	681	4.36	P-n50-k10	650.7	656	0.24
B-n44-k7	833.7	835	1.51	P-n51-k10	698.7	707	0.42
B-n45-k5	698.5	701	16.32	P-n55-k7	546.4	549	5.44
B-n45-k6	656.9	660	5.50	P-n55-k8	569.1	572	6.43
B-n50-k7	679.0	679	2.40	P-n55-k10	666.3	670	3.48
B-n50-k8	1222.5	1224	5.35	P-n55-k15	880.8	889	0.20
B-n51-k7	956.9	961	5.57	P-n60-k10	707.0	712	1.36
B-n52-k7	672.0	675	7.88	P-n60-k15	922.8	931	0.71
B-n56-k7	622.1	623	6.76	P-n65-k10	761.9	765	4.06
B-n57-k7	1052.9	1055	7.99	P-n70-k10	782.4	785	1.44
B-n57-k9	1539.1	1540	4.62	P-n76-k4	589.4	590	98.61
B-n63-k10	1407.0	1407	5.40	P-n76-k5	615.4	616	73.24
B-n64-k9	801.4	803	6.45	P-n101-k4	672.7	673	373.37

* Root LB value correspond to gap 1 value on Table 2.

** Only underlined UB values are not proved to be optimal

Appendix F.4. Raw ILS-VNS results for \mathcal{D}^{card}

Inst.	UB	avg t.	min t.	max t.	Inst.	UB	avg t.	min t.	max t.
A-n32-k5	857	0.27	0.24	0.29	B-n64-k9	865	260.78	38.08	976.54
A-n33-k5	675	0.27	0.25	0.34	B-n66-k9	1319	4.14	1.62	10.42
A-n33-k6	758	0.42	0.25	1.09	B-n67-k10	1086	1.13	0.63	1.68
A-n34-k5	776	0.29	0.28	0.31	B-n68-k9	1298	20.30	2.50	69.54
A-n36-k5	823	0.42	0.30	0.79	B-n78-k10	1261	1305.63	157.17	3065.41
A-n37-k5	706	0.38	0.36	0.40	E-n13-k4	277	0.02	0.02	0.02
A-n37-k6	948	2.76	0.69	9.44	E-n22-k4	373	0.13	0.12	0.13
A-n38-k5	714	0.37	0.36	0.40	E-n23-k3	570	0.23	0.23	0.23
A-n39-k5	818	0.88	0.40	1.74	E-n30-k3	495	0.33	0.32	0.34
A-n39-k6	850	0.63	0.35	0.92	E-n31-k7	379	0.21	0.17	0.23
A-n44-k6	930	0.55	0.45	0.93	E-n33-k4	836	0.37	0.35	0.42
A-n45-k6	918	1.44	0.46	6.10	E-n51-k5	519	1.32	0.69	2.92
A-n45-k7	1163	8.31	0.55	29.40	E-n76-k7	699	5.07	1.85	11.90

A-n46-k7	988	0.52	0.39	0.84	E-n76-k8	736	11.34	1.93	29.46
A-n48-k7	1129	2.91	0.52	9.89	E-n76-k10	830	385.70	66.56	895.89
A-n53-k7	1019	1.91	0.99	4.47	E-n76-k14	1022	171.57	61.57	421.72
A-n54-k7	1169	3.41	0.77	8.77	E-n101-k8	826	25.06	3.41	81.78
A-n55-k9	1107	2.72	1.09	7.46	E-n101-k14	1121	419.22	6.58	1557.43
A-n60-k9	1408	6.62	2.45	12.19	F-n45-k4	736	0.74	0.72	0.78
A-n61-k9	1022	2.55	0.89	4.76	F-n72-k4	236	2.13	2.00	2.26
A-n62-k8	1339	9.73	3.11	18.01	M-n101-k10	918	3.87	1.80	7.70
A-n63-k9	1620	7.85	1.44	23.39	M-n121-k7	1030	8.47	4.58	14.39
A-n63-k10	1348	9.87	1.77	26.70	P-n19-k2	195	0.14	0.14	0.15
A-n64-k9	1417	26.56	4.24	65.36	P-n20-k2	208	0.18	0.18	0.18
A-n65-k9	1184	3.69	1.01	12.21	P-n21-k2	208	0.19	0.19	0.19
A-n69-k9	1177	16.96	4.21	28.54	P-n22-k2	213	0.20	0.20	0.20
A-n80-k10	1803	33.70	6.34	116.94	P-n22-k8	601	0.19	0.12	0.29
B-n31-k5	694	0.23	0.19	0.47	P-n23-k8	527	0.29	0.17	0.47
B-n34-k5	789	0.29	0.27	0.33	P-n40-k5	468	0.47	0.44	0.72
B-n35-k5	986	0.23	0.22	0.26	P-n45-k5	512	2.17	0.51	5.97
B-n38-k6	823	0.32	0.27	0.49	P-n50-k7	563	0.92	0.50	1.48
B-n39-k5	561	0.34	0.30	0.52	P-n50-k8	614	1.32	0.42	2.82
B-n41-k6	838	2.96	0.30	6.36	P-n50-k10	695	3.06	0.98	8.78
B-n43-k6	779	1.69	0.43	2.88	P-n51-k10	736	1.96	0.44	6.52
B-n44-k7	943	0.93	0.46	2.47	P-n55-k7	583	1.98	0.60	3.42
B-n45-k5	739	0.61	0.53	0.74	P-n55-k8	624	2.92	0.80	9.46
B-n45-k6	668	0.38	0.37	0.40	P-n55-k10	718	14.52	1.13	49.25
B-n50-k7	758	1.48	0.44	3.28	P-n55-k15	945	1.91	0.99	3.56
B-n50-k8	1330	24.06	8.89	73.10	P-n60-k10	755	7.40	1.44	19.94
B-n51-k7	1027	2.26	0.54	5.66	P-n60-k15	1020	117.25	37.21	310.22
B-n52-k7	775	0.58	0.45	0.84	P-n65-k10	809	8.17	1.78	18.45
B-n56-k7	740	1.20	0.96	1.75	P-n70-k10	824	37.48	2.81	88.71
B-n57-k7	1132	2.02	0.76	4.79	P-n76-k4	590	7.49	2.33	20.40
B-n57-k9	1656	21.47	4.64	52.27	P-n76-k5	621	4.24	1.77	11.39
B-n63-k10	1588	19.13	2.17	56.77	P-n101-k4	681	6.84	4.50	15.75

Appendix F.5. Raw BCP results for \mathcal{D}^{card}

Inst.	root LB	UB	time	Inst.	root LB	UB	time
A-n32-k5	857.0	857	3.79	B-n64-k9	852.0	<u>866</u>	7200.00
A-n33-k5	675.0	675	6.55	B-n66-k9	1319.0	1319	97.71
A-n33-k6	758.0	758	1.22	B-n67-k10	1086.0	1086	54.20

A-n34-k5	776.0	776	2.26	B-n68-k9	1298.0	1298	63.23
A-n36-k5	823.0	823	7.79	B-n78-k10	1261.0	1261	216.35
A-n37-k5	706.0	706	3.81	E-n13-k4	277.0	277	0.17
A-n37-k6	948.0	948	9.26	E-n22-k4	373.0	373	3.39
A-n38-k5	714.0	714	4.14	E-n23-k3	570.0	570	9.98
A-n39-k5	818.0	818	36.82	E-n30-k3	495.0	495	14.10
A-n39-k6	850.0	850	6.63	E-n31-k7	378.3	379	0.76
A-n44-k6	930.0	930	3.51	E-n33-k4	836.0	836	38.69
A-n45-k6	918.0	918	10.86	E-n51-k5	519.0	519	15.18
A-n45-k7	1163.0	1163	4.85	E-n76-k7	697.0	697	148.17
A-n46-k7	988.0	988	13.18	E-n76-k8	736.0	736	95.75
A-n48-k7	1129.0	1129	47.08	E-n76-k10	830.0	830	200.64
A-n53-k7	1019.0	1019	29.49	E-n76-k14	1020.0	1020	32.34
A-n54-k7	1169.0	1169	53.05	E-n101-k8	826.0	826	909.78
A-n55-k9	1107.0	1107	21.92	E-n101-k14	1107.0	1109	1977.15
A-n60-k9	1404.1	1408	176.50	F-n45-k4	736.0	736	85.10
A-n61-k9	1022.0	1022	34.40	F-n72-k4	236.0	236	583.44
A-n62-k8	1339.0	1339	106.29	M-n101-k10	918.0	918	25.98
A-n63-k9	1612.1	1618	334.82	M-n121-k7	1030.0	1030	450.81
A-n63-k10	1348.0	1348	56.41	P-n19-k2	195.0	195	0.28
A-n64-k9	1413.7	1414	35.36	P-n20-k2	208.0	208	0.52
A-n65-k9	1184.0	1184	91.31	P-n21-k2	208.0	208	0.71
A-n69-k9	1177.0	1177	35.08	P-n22-k2	213.0	213	1.35
A-n80-k10	1795.0	1795	248.47	P-n22-k8	601.0	601	0.75
B-n31-k5	694.0	694	1.36	P-n23-k8	527.0	527	0.24
B-n34-k5	789.0	789	6.44	P-n40-k5	468.0	468	9.59
B-n35-k5	986.0	986	5.37	P-n45-k5	512.0	512	16.64
B-n38-k6	823.0	823	15.59	P-n50-k7	563.0	563	8.01
B-n39-k5	561.0	561	26.39	P-n50-k8	614.0	614	45.16
B-n41-k6	838.0	838	1876.79	P-n50-k10	695.0	695	5.49
B-n43-k6	779.0	779	25.14	P-n51-k10	736.0	736	8.61
B-n44-k7	943.0	943	25.11	P-n55-k7	583.0	583	22.13
B-n45-k5	739.0	739	46.24	P-n55-k8	624.0	624	14.93
B-n45-k6	668.0	668	19.24	P-n55-k10	718.0	718	11.86
B-n50-k7	758.0	758	6.31	P-n55-k15	945.0	945	4.70
B-n50-k8	1330.0	1330	19.70	P-n60-k10	755.0	755	29.65
B-n51-k7	1010.1	<u>1027</u>	7200.00	P-n60-k15	1020.0	1020	20.87
B-n52-k7	775.0	775	22.00	P-n65-k10	809.0	809	66.89

B-n56-k7	740.0	740	23.78	P-n70-k10	824.0	824	63.11
B-n57-k7	1112.8	<u>1133</u>	7200.00	P-n76-k4	590.0	590	267.42
B-n57-k9	1656.0	1656	77.70	P-n76-k5	621.0	621	284.10
B-n63-k10	1578.9	1587	843.21	P-n101-k4	681.0	681	2096.77

* Root LB value correspond to gap 1 value on Table 4.

** Only underlined UB values are not proved to be optimal